The Intrinsically Disordered Region of ExbD is Required for Signal Transduction.

Dale R. Kopp[1] and Kathleen Postle[*]

Running title: *ExbD-TonB interactions*

Keywords: TonB, ExbD, intrinsic disorder, binding motif, energy transduction

[1]Department of Biochemistry and Molecular Biology, The Pennsylvania State University, University Park, PA, 16802, USA

* Correspondence:

Kathleen Postle, Department of Biochemistry and Molecular Biology, The Pennsylvania State University, University Park, PA 16802, USA. email: postle@psu.edu, Ph. 1-814-863-7568, Fx. 1-814-863-7024

ABSTRACT:

In most Gram-negative bacteria, the TonB system is required to actively transport vital nutrients across their unenergized outer-membrane barriers. The cytoplasmic membrane proteins of the system ExbB, ExbD, and TonB work together to transduce the energy from the protonmotive force (PMF) of the inner membrane to the ligand-specific, outer membrane TonB-dependent transporters. However, the precise coordination and interactions between ExbB, ExbD, and TonB during energy transduction is unclear. Previously, deletions within a periplasmic disordered domain of ExbD had been shown to be important for TonB system activity and the essential ExbD-TonB PMF-dependent interaction. In this study, we have discovered a conserved motif, ΨXΨXLP (Ψ = hydrophobic-branched residues; X = non-hydrophobic residues) specifically within this domain that was required for both TonB system function and the ExbD-TonB PMF-dependent interaction. Alanine scanning mutagenesis found that the only functionally important residues within the ExbD disordered domain were those located in the motif. In addition, *in vivo* photo-cross-linking captured and identified five ExbD complexes from pBpa substitutions within the ExbD disordered domain: 2-ExbB-ExbD complexes, the ExbD homodimer, the PMF-dependent ExbD-TonB, and the first captured, ExbD-TonB *in*dependent interaction. Interestingly, many of these complexes were captured from single pBpa substitutions, which suggests that these residues are involved in multiple interactions. The data presented in this study indicate that the ExbD disordered domain is a highly dynamic region *in vivo* and a conserved motif within this domain is required for the TonB system to respond to protonmotive force.

48 **Importance:**

49 Within the context of pathogenicity, the TonB system is a virulence factor in many
50 Gram-negative pathogens including E-S-K-A-P-E pathogenic species *Klebsiella pneumoniae*,
51 *Acinetobacter baumannii*, *and Pseudomonas aeruginosa*. Because the TonB system is unique
52 to Gram-negative bacteria and is a periplasmically localized virulence factor, it is an appealing
53 target for novel antibiotics. However, there is no current antibiotic against this system.
54 Understanding the mechanism by which the TonB system functions will provide valuable
55 information to design potential inhibitors targeting the system.

56

57

58

59

60

61

62

63

64

65

66

67

68

69 **INTRODUCTION:**

70 The TonB system is required for most Gram-negative bacteria to acquire vital nutrients
71 such iron, vitamin B_{12}, nickel, cobalt, copper, heme, maltodextrin, and sucrose across their
72 outer-membrane barriers (1), and is major virulence factor in many pathogenic Gram-negative
73 bacteria (2, 3). Under iron-limiting conditions, such as the human serum (3), Gram-negative
74 bacteria secrete iron-chelating compounds called siderophores that capture the iron with high
75 affinity. However, because iron-siderophore complexes are too large, too scare, and too
76 important to passively diffuse through the outer-membrane porins, they require customized 22-
77 stranded beta-barrel transporters called TonB-dependent transporters (TBDTs) to transition
78 across the outer-membrane (1, 4, 5). After the siderophore captures an iron atom
79 extracellularly, the iron-siderophore complex binds to a TDBT with sub-nanomolar affinity,
80 causing the ligand-loaded TBDT to signal on its periplasmic face that ligand is bound (6–9).
81 Energy is required to release the iron-siderophore from the TBDT (1–3). Because the outer-
82 membrane and periplasmic space lack a sufficient energy source, Gram-negative bacteria
83 transduce the energy from the cytoplasmic membrane proton motive force (PMF) to the TBDTs
84 using the three integral cytoplasmic membrane proteins of the TonB system--ExbB, ExbD, and
85 TonB (12, 13).

86 In *Escherichia coli K-12*, there are six TBDTs that transport various sources of iron and
87 one TBDT that transports vitamin B12 (4). With a cellular ratio of 7 ExbB: 2 ExbD: 1 TonB,
88 ExbB and ExbD through an unclear mechanism harvest the PMF and transmit it to TonB (14).
89 ExbB has three transmembrane domains (TMDs) with majority of the protein residing in the
90 cytoplasm [Fig. 1, (15, 16)]. In contrast, ExbD and TonB are anchored by single N-terminal
91 TMDs with the bulk of their residues occupying the periplasm (17, 18). ExbB, ExbD, and TonB
92 also share homology through their TMDs with proteins TolQ, TolR, and TolA of the Tol system,
93 which is necessary for outer membrane integrity and important for cell division (19–21). Both

94 systems are energized by PMF, suggesting that they have a common means of PMF utilization
95 that plays out as different roles in cell physiology due to different protein contacts made by
96 their soluble domains (22, 23).

97 Because the TBDTs greatly outnumber the molecules of TonB per cell (14) and there is
98 competition between TBDTs for “energized” TonB (24), TonB must undergo a cyclic pattern of
99 binding and release from TBDT to TBDT (8, 25). This pattern is referred to as the TonB
100 energization cycle (26). TonB binds to TBDTs both *in vitro* and *in vivo* whether or not it is
101 “energized”, and therefore, it must be correctly configured during an energy transduction cycle
102 to enable productive interaction with the TBDT (6, 27–29). Both ExbB and ExbD are required
103 to correctly configure TonB to energize active transport across the outer membrane--ExbB
104 indirectly, and ExbD directly (16, 30, 31).

105 ExbB serves as a scaffolding protein for ExbD and TonB assembly, without which they
106 are both proteolytically unstable, and mediates ExbD-TonB interactions (16, 30–33). The
107 ExbD-TonB interactions, or lack thereof, define our model for the initial Stages of the TonB
108 energization cycle (26, 34). In Stage I, ExbD and TonB homodimers exist in separate
109 complexes with ExbB, but do not interact (26). To transition to Stage II, ExbB facilitates
110 bringing ExbD and TonB homodimers together in a single complex to form PMF-independent
111 ExbD-TonB interactions. The PMF-independent ExbD-TonB interaction has only been
112 detected indirectly by the protection from ExbD of the N-terminal ~155 residues of TonB in the
113 of proteinase K. A proteinase K-resistant conformation of TonB exists in spheroplasts that
114 requires a functional ExbD protein and accumulates in the absence of PMF (34, 35, 16). In the
115 presence of PMF, the ExbD and TonB homodimers swap partners to form PMF-dependent
116 ExbD-TonB heterodimers which is identified as Stage III. In this Stage, the PMF-dependent
117 ExbD-TonB interaction can be captured with formaldehyde *in vivo* (31). The only TMD among

118 the cytoplasmic membrane proteins of the TonB system that can participate in response to
119 PMF is ExbD, with its D25 residue (16, 31, 36).

120 ExbD has five structurally distinct domains: a cytoplasmically localized N-terminus
121 (residues 1-22), a predicted TMD (residues 23-43), a disordered periplasmic domain (44-63), a
122 structured periplasmic domain (residues 64-133) and a flexible C-terminus (residues 134-141)
123 (37). Experiments using *in vivo* disulfide cross-linking of engineered Cys residues in the ExbD
124 and TonB distal periplasmic domains are consistent with the three-Stage model. The same
125 ExbD residues in the region of 92-121 that form a homodimeric interface are almost the exact
126 same residues that form ExbD-TonB heterodimers through the TonB periplasmic domain (38).
127 Also, in a PMF-unresponsive ExbD mutant, ExbD (D25N), ExbD-TonB disulfide cross-links are
128 either absent or significantly reduced (39).

129 A 10 residue-deletion scanning mutagenesis of ExbD revealed that deletions within
130 ExbD periplasmic residues 62-141 stall TonB energization in Stage I, whereas deletions
131 largely encompassing the disordered domain of ExbD (42-61) stall TonB energization in Stage
132 II, unable to proceed to Stage III. However, it was unclear how the disordered domain of ExbD
133 participated in energy transduction.

134 Here we discovered that a novel periplasmic motif, ΨXΨXLP (Ψ = hydrophobic-
135 branched residues; X = non-hydrophobic residues) located very near the ExbD TMD, is
136 essential for ExbD activity. This motif within the disordered domain of ExbD is required for
137 transition from Stage II to Stage III and may account for crosstalk between the TonB and Tol
138 systems because it also exists in TolR. More broadly, the disordered domain makes contacts
139 with another ExbD and with ExbB through two different sites or conformations. Importantly, the
140 disordered domain also forms the long-predicted PMF-*in*dependent complex between ExbD
141 and TonB, visualized for the first time without requiring collapse of PMF, indicating it is part of

142 the normal energy transduction cycle. It also forms the PMF-dependent complex previously
143 visualized by formaldehyde cross-linking. This study thus identifies for the first time, at least
144 one of the ExbD domains and its contacts involved in TonB-dependent energy transduction.
145

146 **RESULTS:**

147 **Within the ExbD disordered domain, residues 44-53 are essential for TonB system**
148 **activity.**

149 In our previous study, deletions that encompassed most of the disordered domain of
150 ExbD protein, (Δ42-51) and (Δ52-61), were completely inactive because they eliminated the
151 ability of its partner protein, TonB, to undergo essential conformational changes in response to
152 change in PMF (35, 37). The effects of these deletions could have been due to structural
153 distortions. To circumvent that issue, here we engineered and characterized ExbD with blocks
154 of alanine substitutions to identify functionally important residues within the disordered domain
155 (Fig. 1B): ExbD (44-48ala), ExbD (49-53ala), ExbD (54-58ala), and ExbD (59-63ala). TonB
156 system activity was determined by measuring the initial transport rates of two different iron-
157 siderophores, ^{55}Fe-enterochelin and ^{55}Fe-ferrichrome (6, 40), to identify any TonB-dependent
158 transporter-specific activities.

159 While both ExbD (54-58ala) and ExbD (59-63ala) transported ^{55}Fe-enterochelin or ^{55}Fe-
160 ferrichrome at rates equivalent to the wild-type ExbD encoded on pKP999 (pExbD), neither
161 ExbD (44-48ala) nor ExbD (49-53ala) were able to transport either siderophore. ExbD (59-
162 63ala) required significantly more sodium propionate (20 mM) to achieve chromosomal ExbD
163 levels, suggesting that it was important for proteolytic stability (Fig. 2). These results excluded
164 residues 54-63 as functionally important for the TonB system and eliminated the possibility of
165 siderophore-specific effects.

166 Previously, ExbD (Δ42-51) and ExbD (Δ52-61) were unable to form the formaldehyde-
167 cross-linked ExbD-TonB complex that typifies Stage III (35). Consistent with that, the inactive
168 ExbD (44-48ala) and ExbD (49-53ala) had the same cross-linking profile in the presence and
169 absence of TonB, whereas for the active ExbD (54-58ala), and ExbD (59-63ala), the absence
170 of TonB led to the absence of the formaldehyde cross-linked ExbD-TonB complex (Fig. S1).

171 To test whether the absence of the PMF-dependent ExbD-TonB complex was due to
172 the ability of ExbD (44-48ala) and ExbD (49-53ala) to somehow induce proton leakage, we
173 measured the rate of PMF-dependent ethidium bromide efflux through the AcrA/AcrB/TolC
174 complex (41, 42). None of the block ala mutants came close to PMF leakage caused by 15 μM
175 CCCP, which nonetheless still supports 100% ^{55}Fe-ferrichrome transport (data not shown)
176 (Fig. S2A). Because PMF was adequate for ^{55}Fe-ferrichrome transport, the reason for the
177 inactivity of the block ala substitutions must lie elsewhere.

178 Expression of ExbD (44-48ala) did, however, cause a small but statistically significant
179 increase in ethidium bromide accumulation compared to pExbD (Fig. S2B). The means by
180 which ExbD (44-48ala) caused this low level of proton leakage was unclear, especially since
181 the Δ*exbD* strain with *tolQR* present did not detectably leak protons (data not shown). Because
182 there is crosstalk between the TonB system and the Tol-Pal system (43), and because
183 RA1045 (Δ*exbD*, Δ*tolQR*) showed the same degree of proton leakage as ExbD (44-48ala), we
184 speculate that protons could possibly have been leaking through TolA in the absence of TolQR
185 or a functional ExbBD.

186 ***In vivo* photo-cross-linking identifies characteristic PMF-dependent and novel PMF-**
187 **independent ExbD-TonB complexes.**

188 Disordered domains of proteins are often regions of interaction with other proteins. In
189 the case of ExbD and TonB, both of which contain regions of disorder, we know that they

190 formaldehyde-cross-link, but the residues involved in either protein are unknown. To identify
191 contacts made by the ExbD disordered domain, individual amber mutations were constructed
192 at codons 44-63 for *in vivo* photo-cross-linking. For *in vivo* photo-cross-linking, the
193 photoreactive, non-natural amino acid, *p*-benzoyl-L-phenylalanine (*p*Bpa) is incorporated at the
194 site of an amber mutation and can covalently capture protein interactions within 3 angstroms
195 upon exposure to ultraviolet (UV) light (44). The advantage of this approach over formaldehyde
196 cross-linking is that interactions through defined sites can be investigated, while leaving the
197 positions of residues in binding partners unconstrained.

198 To characterize ExbD-TonB interactions made through the ExbD disordered domain, we
199 chose ExbD (S54pBpa) and ExbD (R59pBpa) as representatives. Both variants were active in
200 iron transport assays and shared representative complexes with the rest of the pBpa
201 substitution mutants (shown below). On immunoblots developed with anti-TonB monoclonal
202 antibodies, two different ExbD-TonB complexes were captured by both variants, a doublet at
203 ~55 kDa and a single band at ~46 kDa (Fig. 2, lanes 4 and 8). Because a C-terminally added
204 His6X epitope tag caused each of the complexes to migrate at a higher apparent mass
205 equivalent to that of the added His6X tag, all the bands consisted of TonB complexed with full-
206 length ExbD (Fig. 2, lanes 11 and 12). No complexes were detected in a strain where the *tonB*
207 gene was deleted (Fig. 2, lane 7).

208 The sole potentially proton-responsive amino acid in the TonB system, Asp 25, resides
209 in the TMD of ExbD [Fig. 1,(16, 36)]. ExbD (D25N) is a well-characterized inactive mutant
210 which causes the TonB energization cycle to stall at Stage II and is therefore useful for
211 differentiating between PMF- dependent and -independent ExbD interactions (45, 31, 34, 38).
212 Complexes decreased or eliminated by ExbD (S54pBpa) and ExbD (R59pBpa) in concert with
213 the D25N mutation (Fig. 2, lanes 5 and 9) or by treatment with the protonophore CCCP (Fig. 2,

214 lanes 6 and 10) identified the 55 kDa doublet as being PMF-dependent. Although the reason
215 for the doublet is not clear, it could represent two different PMF-dependent sites of contact
216 made by ExbD (S54pBpa) and ExbD (R59pBpa) with TonB.

217 In contrast, the abundance of 46 kDa ExbD-TonB complex was undiminished by the
218 presence of the ExbD D25N mutation or by CCCP treatment, indicating that is was a PMF-
219 independent complex. If anything, the ExbD D25N mutation generated higher levels of the 46
220 kDa complex, consistent with the idea that it stalls TonB at Stage II, where such complexes
221 could build up. These data were also consistent with our finding that in Stage II of TonB
222 energization, ExbD protects the first ~155 residues of TonB from degradation by proteinase K
223 in the absence of PMF (34). They also verified that loss of PMF causes a significant and, now
224 detectable, change in the sites through which ExbD disordered domain residues contact
225 TonB—enough difference that it results in significant change in apparent mass of the complex
226 from 55 kDa to 46 kDa.

227 While we knew that ExbD and TonB made *in vivo* contacts through their extreme C-
228 termini, many of them beyond the N-terminal ~155 residues of TonB (38, 39), we did not know
229 that additional ExbD contacts occurred so close to the ExbD (and, presumably, TonB) TMDs
230 (Fig. 1A,B).

231 **Most of the pBpa substitutions in the ExbD disordered domain capture some form of**
232 **TonB contact.**

233 To understand the full extent of interactions between the ExbD disordered domain and
234 TonB, *in vivo* photo-cross-linking was carried out through pBpa substitutions at ExbD codons
235 44-63. Most pBpa substitutions in the region from 44-52 supported significantly reduced TonB-
236 dependent ^{55}Fe transport activity (< 25% wild-type levels), consistent with the results from the
237 block ala substitutions which essentially eliminated activity (Fig. 4A). Substitutions at residues

238 53-63 all supported at least 50% activity except for ExbD (R59pBpa) which also supported only
239 25% activity. Several single pBpa substitution mutants from residues 54-63 were less active
240 than ExbD (54-58ala) and ExbD (59-63ala) (compare Fig. 2A with Fig. 4A, right panel). The
241 bulky pBpa side chain was likely responsible for the discrepancy, possibly alluding to the
242 importance of conformational flexibility or lock and key fit for these residues. Nonetheless,
243 except for ExbD (V45pBpa) and ExbD (V47pBpa), all the pBpa substitutions within the ExbD
244 disordered domain had detectable levels of activity. Therefore, the complexes captured by
245 these substitutions at least indicated TonB proteins within ~3angstroms of the pBpa moiety
246 (46) and likely reflected interactions that occurred during a TonB energization cycle.

247 The PMF-dependent ExbD-TonB complexes formed starting at approximately ExbD
248 residue A51(pBpa) and continuing through P63 (pBpa), with all the pBpa substitutions except
249 S52(pBpa) participating (Fig. 4B). Consistent with the predicted intrinsically disordered nature
250 of this region (35, 37), there was not a strong pattern of interaction suggestive of an α-helix or
251 β-sheet.

252 We had previously observed a PMF-dependent formaldehyde-cross-linked ExbD-TonB
253 complex, but did not know through which residues of the ExbD periplasmic domain it occurred
254 (31). The ExbD disordered domain contains only three formaldehyde-cross-linkable residues:
255 K46, R59, and K62 (47). Because ExbD (K46pBpa) was unable to capture the PMF-dependent
256 ExbD-TonB interaction via photo-cross-linking (Fig. 4B, left panel) and ExbD (59-63ala) still
257 captured the PMF-dependent formaldehyde-cross-linked ExbD-TonB complex (Fig. S1), the
258 idea that the ExbD disordered domain participated in the previously observed PMF-dependent
259 formaldehyde cross-link to TonB could be ruled out.

260 The PMF-independent ExbD-TonB interaction characterized in Fig. 3, was captured by
261 most of the residues within the ExbD disordered domain (Fig. 4B). Because the abundance of

262 complex was fainter at either end of the range of pBpa substitutions, it could be that the ExbD
263 disordered domain constituted the PMF-independent interface. Interestingly, the ExbD
264 disordered residues that trapped the PMF-independent interactions were similar to an ExbD
265 interface predicted to interact with TonB by phage-panning experiments (46-62) (48).

266 In addition to the ExbD-TonB PMF-dependent complex and ExbD-TonB PMF-
267 independent complex, there was also an unknown ~62 kDa complex trapped via photo-cross-
268 linking by ExbD (T53pBpa) and ExbD (Q57pBpa) (Fig. 4B). We do not know the identity of the
269 complex except that it certainly contains both ExbD and TonB.

270 **The ExbD disordered domain interacts with ExbB and another ExbD.**

271 ExbD formaldehyde- cross-links *in vivo* into a single homodimeric complex (~ 30 kDa)
272 and a single heterodimeric complex with ExbB (~41 kDa) through unknown residues (31, 34).
273 To determine if the ExbD disordered domain formed such complexes, we used ExbD
274 (D44pBpa) and (S54pBpa) as examples (Fig. 5A, B). In Fig. 5A, ExbD (D44 pBpa) formed
275 complexes with apparent masses of ~39 kDa and ~43 kDa, making them both, based on their
276 apparent masses, candidates to be potential ExbD-ExbB complexes. Surprisingly, the addition
277 of a His6X-tag caused both complexes to shift to a higher mass consistent with the added
278 His6X tag, indicating that both were ExbD-ExbB complexes. The presence of two different
279 ExbD-ExbB complexes indicated that either or both proteins were undergoing conformational
280 changes that influenced the nature of the contacts between them during the energy
281 transduction cycle.

282 In Fig. 5B, ExbD (S54pBpa) formed an ~31 kDa complex. A C-terminal His6X tag
283 caused the 31 kDa complex to migrate 1.2 kDa more slowly, twice the effect of the His 6X tag
284 on the apparent mass of the ExbD monomer (Fig. 5B). Thus the ~31 kDa complex was
285 identified as an ExbD homodimer. ExbD (S54pBpa) also formed the lower of the two ExbD-

286 ExbB complexes and, as expected, the ExbD-TonB PMF-dependent and -independent
287 complexes.

288 **The majority of pBpa substitutions in the ExbD disordered domain capture contacts**
289 **with ExbB as well as ExbD.**

290 To understand the full extent of interaction between the ExbD disordered domain and
291 itself or ExbB, we analyzed *in vivo* photo-cross-linking by the series of ExbD (pBpa)
292 substitutions by immunoblot with anti-ExbD antibody. As expected, the ExbD-TonB PMF-
293 dependent and -independent complexes could be discerned, but they were less confidently
294 identified due to the presence of other complexes in the same region of the immunoblot,
295 indicating that ExbD interacted with additional proteins, as seen in Fig. 5.

296 The ExbB-ExbD (upper, ~43 kDa) complex was prominently formed by residues from
297 the beginning of the ExbD disordered domain D44pBpa until P50pBpa, contacts that placed
298 the region just distal to the ExbD TMD close to ExbB (Fig.1). It is likely that ExbD pBpa 46-50
299 lanes (Fig. 6, lanes 5-10) also contain ExbD-TonB PMF-independent complex, which runs
300 similarly to the ExbB-ExbD (upper, ~43 kDa) complex (compare to Fig. 4 lanes 5-10) and is
301 therefore difficult to separately identify.

302 The ~ 39 kDa ExbD-ExbB (lower) complex was formed by pBpa substitutions
303 throughout the disordered domain from D44 through P63 at similar intensities. This indicates
304 that a site in ExbD ~20 residues from its predicted periplasmic TMD boundary [residues 32-43,
305 (15)] binds to ExbB. The fact that ExbB has only a 20 residue periplasmic loop and a 21-
306 residue periplasmic amino terminus (13), raises the possibility that the ExbD disordered
307 domain was condensed at some point during the TonB energization cycle such that it was
308 closer to the inner-membrane. Alternatively, the ExbB periplasmic terminus might extend,
309 structureless, into the periplasm.

310 In contrast to the ExbD-TonB complexes, the ExbD-ExbD homodimers were captured
311 more efficiently in the mutation-intolerant half of the ExbD disordered domain, residues 44-49
312 and 52-55, without emergence of a pattern indicative of structural elements.

313 **The ExbD disordered domain contains a ΨXΨXLP motif.**

314 A multiple sequence alignment of the ExbD disordered domain was generated and
315 displayed in a sequence logo using HHblits in the Gremelin.bakerlab program of all sequences
316 within an expect score of e^{-10} of *Escherichia coli K-12 strain* (NP_417478.1) (Fig. 7A). The
317 sequence logo identified a ΨXΨXLP motif where the psi symbol (Ψ) represents large aliphatic
318 side-chained residues, (11) and X represents any non-hydrophobic residue (Fig. 7B). The motif
319 includes residues V45, V47, L49, and P50, which reside in the mutation-intolerant segment of
320 the disordered domain and are also conserved in the *Escherichia coli* ExbD paralog, TolR of
321 the Tol system, but not in paralog MotB of the flagellar motor (Fig. 7B). Due to the similarities
322 between ExbB/ExbD TMDs of the TonB system and TolQ/TolR TMDs of the Tol system, there
323 is modest crosstalk between the two systems such that they can substitute functionally for one
324 another (43, 49). To our knowledge, MotAB has not been shown to account for any crosstalk. Its
325 conservation in TolR and ExbD suggests the ΨXΨXLP motif may have a shared function in
326 both proteins, and could account for the cross-talk between ExbB/ExbD and TolQ/R (43, 49, 50).

327 **Only ExbD motif residues V45, V47, L49 and P50 are important for TonB system activity.**

328 Assessment of the activities of the pBpa substitutions in the mutation-intolerant segment
329 showed that the least active ones [V45(pBpa) and V47(pBpa)], were part of the ΨXΨXLP motif
330 (Fig. 4A). To better define the motif, individual alanine substitutions were constructed in ExbD
331 from residues 44 through 53. ExbD variants carrying V45A, V47A. L49A, and P50A mutations
332 were the only ones with deficits in initial ^{55}Fe-ferrichrome transport rates significantly below
333 90% of pExbD, with activities of 32%, 21%, 34%, and 50%, respectively (Fig. S3). Thus V45,

334 V47, L49 and P50 were the only functionally important residues within the entire ExbD
335 disordered domain.

336 To further define the motif, each of the V45A, V47A, L49A, and P50A substitutions in
337 the motif region was combined with the others to create six double ala substitutions. Had these
338 mutations been simply additive in their effects, we would have seen that, for example, the
339 V45A, P50A double mutant should have ~16% activity (50% of 32%). Instead, this double
340 mutant, like all six double mutants, was inactive in ^{55}Fe-ferrichrome transport, suggesting a
341 degree of synergy between them (Fig. 8A). However, the iron transport assays are not
342 sensitive to very low levels of TonB system activity (51).

343 Colicins toxins are synthesized by some *E. coli* to kill sensitive strains. B-group colicins
344 all use the TonB system to cross the outer membrane of *E. coli* to gain access to their targets
345 in the periplasm, cytoplasmic membrane or cytoplasm (52) Colicin sensitivity assays, while not
346 as discriminative among higher levels of TonB system activity, can detect the activity
347 supported by as little as one molecule of TonB (51). To determine whether the double ala
348 substitutions could support any activity, their sensitivity to B-group colicins B, Ia, and M was
349 tested (Fig. 8B). All of the double-ala mutants were tolerant (insensitive) to virtually all colicins
350 tested, indicating that they do not work independently of each other and validating the
351 identification of this motif.

352 **ExbD (V45A, V47A), ExbD (V47A, L49A), and ExbD (L49A, P50A) stall TonB at Stage II of**
353 **the energy transduction cycle.**

354 ExbD regulates TonB conformational changes as TonB moves through an energy
355 transduction cycle (34). Stage II of the TonB energization cycle is a PMF-independent Stage
356 where the N-terminal ~ 155 residues of TonB (an ~23 kDa fragment) are protected from
357 proteinase K degradation if full-length ExbD is present, although an actual complex between

358 the two proteins had not been observed until this study (Fig. 5). Heretofore, Stage II had been
359 detectable only when PMF was collapsed, preventing TonB from moving on to Stage III. When
360 PMF, ExbB, ExbD, and TonB are all present and active, TonB transitions from Stage II to
361 Stage III, rendering TonB fully sensitive to proteinase-K. Our observation that ExbD (44-48ala)
362 and ExbD (49-53ala) failed to form a Stage III formaldehyde cross-link suggested that the
363 effects of substitutions in the disordered domain motif might be to stall TonB at Stage II [Fig.
364 S1,(34)]. Since only ExbD residues V45, V47, L49, and P50 were important for ExbD activity,
365 we assessed whether the inactive double mutants (V45A, V47A), (V47A, L49A) and (L49A,
366 P50A) were required for TonB to proceed beyond Stage II based on its sensitivity to
367 exogenously added proteinase K in spheroplasts. For comparison, we assessed ExbD (D25N).

368 The hallmarks of the ExbD (D25N) mutant, where TonB is permanently stalled at Stage
369 II are 1) that TonB forms a proteinase K-resistant fragment in both the presence and absence
370 of CCCP and 2) that TonB is unable to remain in its stalled Stage II proteinase K-resistant
371 conformation over time [Fig. 8, panel 4 +/- CCCP; (34)]. As expected, the Δ*exbD,* Δ*tolQR*
372 strain did not support the ability of TonB to form the ~23 kDa proteinase K-resistant TonB
373 fragment [Fig. 8, panel 3; (34)]. A ~28 kDa TonB fragment, seen previously and typified by
374 Δ*exbD,* Δ*tolQR* and ExbD (D25N) in panels 3 and 4, does not appear to have relevance to the
375 mechanism of TonB energization (34).

376 ExbD (V45A, V47A) and ExbD (V47A, L49A) largely mimicked the effect of ExbD
377 (D25N) on TonB, leaving it stalled in Stage II (Fig. 9). ExbD (L49A, P50A) was too sensitive to
378 proteinase K to be evaluated (Fig. 9 panel 7). Together the results suggest that the ExbD
379 ΨXΨXLP motif was required for TonB to transition from Stage II to Stage III of the energization
380 cycle.

381 **The ExbD disordered domain ΨXΨXLP motif is required for correct configuration of the**
382 **ExbD C-terminus.**

383 To better understand why the ExbD ΨXΨXLP motif left TonB stalled in Stage II, we
384 combined the V45A, V47A double mutation with pBpa substitutions along the length of ExbD:
385 E14(pBpa)— presumably cytoplasmically localized based on the topology of ExbD;
386 I24(pBpa)—in the TMD; S54(pBpa)—in the mutation-tolerant segment of the disordered
387 domain S67(pBpa)—just beyond the disordered domain K97(pBpa)—a known point of ExbD-
388 TonB contact and E136(pBpa)—near the C-terminus. With the exception of ExbD (I24pBpa),
389 the other substitutions were active [ExbD E14pBpa, S67pBpa, K97pBpa, and E136pBpa
390 substitutions were 72%, 24%, 90%, and 100% of ^{55}Fe-Ferrichrome transport of pKP999 +
391 pEVOL in RA1045 (data not shown)].

392 Overall, the double V45A, V47A substitutions did not have much effect on ExbD photo-
393 cross-links to TonB through distal pBpa substitutions, except for (S54pBpa) where it greatly
394 diminished a PMF-dependent ExbD-TonB complex (Fig. 10A lanes 6,7). ExbD (E14pBpa), in
395 the cytoplasm, did not form complexes with TonB (Fig. 10A, lanes 4,5), however, ExbD
396 (I24pBpa), in the TMD, formed a PMF-independent TonB complex (10A lanes 6,7), indicating
397 that at some point in its energy transduction cycle, TonB was in close proximity to ExbD
398 through their TMDs. ExbD (K97pBpa) and ExbD (E136pBpa) also formed PMF-independent
399 Stage II complexes with TonB (Fig. 10A, lanes 6,7,12-15). We do not know why the level of
400 monomer was consistently reduced for ExbD (K97pBpa), but it clearly did not prevent capture
401 of ExbD-TonB complexes.

402 Among the periplasmic pBpa substitutions tested, the presence of the V45A, V47A
403 double substitution caused ExbD to photo-cross-link to a variety of unknown proteins,
404 especially ExbD (S54pBpa) V45A,V47A, which captured at least six different complexes with

405 unknown proteins (Fig. 10B, lane 24). Furthermore, ExbD (E136pBpa) V45A,V47A captured
406 two prominent complexes with unknown proteins. These results showed that the disordered
407 domain of ExbD was important for regulating the ExbD C-terminal conformation and contacts.

408 The V45A, V47A mutations within ExbD show a protein-wide alteration of ExbD residue
409 contacts. In many cases, the mutations reduced distal ExbD residue interactions with TonB
410 and caused additional unknown complex formations. This demonstrates a tight connection
411 between the ΨXΨXLP motif and the distant ExbD C-terminal residues, and potentially
412 highlights a protein-wide functional role of the ΨXΨXLP motif in signal transduction.

413

414 **DISCUSSION:**

415 Understanding the molecular interactions among TonB system proteins in the
416 cytoplasmic membrane--ExbB, ExbD, TonB--and the TBDTs in the outer membrane is vital to
417 our understanding its mechanism. TonB-dependent energy transduction is cyclic, with TonB
418 engaging and disengaging from a TBDT as it energizes active transport across the OM.

419 Our current model has identified multiple stages that occur before the signal
420 transduction from the TonB system cytoplasmic membrane proteins to the TBDT is completed
421 [(26), Figure 12]. In Stage I, TonB and ExbD homodimers are each found in separate
422 complexes with ExbB homotetramers and they do not interact. In Stage II, the ExbB-TonB and
423 ExbB-ExbD complexes come together to form a multimeric heterocomplex in which ExbD
424 protects the first ~155 residues of TonB from digestion by proteinase K in spheroplasts. Prior
425 to this study, we had not been able to determine precisely through which residues the PMF-
426 independent Stage II complex forms. Nor had we been able to observe the TonB and ExbD
427 proteins complexed together in Stage II, although their existence was predicted by the model.
428 From Stage II the TonB system transitions to Stage III, characterized by a requirement for PMF

429 and a formaldehyde- cross-linked complex containing both proteins. The final Stage in our
430 current model is Stage IV in which reconfigured TonB binds the TBDT in such a manner that
431 active transport across the OM occurs. After Stage IV, the multimeric heterocomplex of ExbB,
432 ExbD, and TonB breaks down into isolated complexes of ExbB-ExbD, ExbB-TonB, and free-
433 floating ExbB (26).

434 **The ExbD-TonB, ExbB-ExbD, and ExbD homodimeric complexes identified within the**
435 **ExbD disordered domain.**

436 *In vivo* photo-cross-linking has the advantage of potentially capturing every interaction
437 within ~3 angstroms that a single residue, as a pBpa substitution, is involved with during the
438 TonB energization cycle (46). Throughout the ExbD disordered domain (residues 44-63
439 immediately distal to its TMD), each single ExbD residue captured multiple complexes
440 suggesting that it was a highly dynamic region. Disordered domains of proteins are known to
441 have a high degree of conformational plasticity that can dictate changes in protein
442 oligomerization and function (53). For example, the *E. coli* periplasmic protease/chaperone,
443 DegP, upon substrate binding to its intrinsically disordered domain, it changes from
444 proteolytically inactive hexamers to proteolytically active large polyhedrons consisting of 4, 6,
445 and,8 trimers (54, 55). Most of the ExbD pBpa substitutions within the disordered domain
446 captured at least four of the five identifiable complexes (ExbD homodimer, two ExbD-ExbB
447 complexes, and two ExbD-TonB complexes) through a single site. This indicated that residues
448 within the ExbD disordered domain must have undergone multiple partner swaps during the
449 TonB energization cycle and demonstrated the minimum number of disordered domain
450 contacts that occurred.

451 *ExbD-TonB complexes* – Residues within the ExbD disordered domain, as pBpa
452 substitutions, captured both PMF-independent and PMF-dependent ExbD-TonB interactions
453 using *in vivo* photo-cross-linking. The PMF-independent ExbD-TonB complex was captured by

454 ExbD disordered residues 45-63. It was the first time that this interaction was captured,
455 demonstrating the previously predicted existence of Stage II in the TonB energization cycle,
456 and identified residues through which this complex is formed. Previous residue-specific
457 disulfide experiments within the ExbD 92-121 residues did not trap the PMF-independent
458 interaction. It may be because the PMF-independent interaction mostly, albeit not entirely,
459 occurs with ExbD residues closest to the membrane which would explain why the TonB portion
460 that is protected by Proteinase K is that closest to its TMD. However, the number of residues
461 within ExbD disordered domain (20 amino acids) that trap this interaction is disproportional to
462 that of the periplasmic portion of TonB protected against proteinase K degradation (~123
463 amino acids). It is possible that the full ExbD periplasmic domain contributes to the protection
464 of TonB, but the PMF-independent interface is more localized. Consistent with this idea is that
465 the portion of TonB that is protected by proteinase K is similar to the length of the entire ExbD
466 periplasmic domain. Furthermore, the PMF-independent ExbD-TonB interaction is also
467 captured from distal ExbD C-terminal residues. Alternatively, the ExbD disordered domain may
468 induce a conformational change in the TonB predicted disordered domain (~118 amino acids)
469 to an ordered conformation, which in turn is protected from proteinase K (56). The idea that
470 ExbD could possibly influence TonB to transition from a disordered to ordered state has been
471 previously proposed (23, 57).

472 PMF-dependent ExbD-TonB complexes were captured from ExbD residue A51 to P63
473 (except for S52). Although deletions within the ExbD disordered domain confirmed its
474 importance for forming the ExbD-TonB PMF-dependent interaction, we showed here that the
475 ExbD disordered domain directly contacted TonB PMF-dependently. Thus, we identified
476 another ExbD region besides residues 92-121 can interact with TonB PMF-dependently.
477 However, like the ExbD region of 92-121 cysteine substitutions, alanine substitutions for the

478 ExbD disordered domain residues that captured the PMF-dependent ExbD-TonB interaction
479 did not significantly affect TonB system activity. Therefore, these specific residues are
480 dispensable and are not individually important TonB function. This may suggest that an ExbD
481 region(s) other than the disordered domain and the 92-121 residue region contains the
482 functionally important ExbD residues for the PMF-dependent ExbD-TonB interaction. It also
483 cannot be ruled out that some functionally important ExbD disordered residues (i.e. V45 and
484 V47) directly interact with TonB PMF-dependently, but due to low activity, the interaction was
485 not captured.

486 *ExbD-ExbB complexes* - Two distinct ExbD-ExbB complexes were captured via photo-
487 cross-linking: an ~ 39 kDa (lower) complex and an ~43 kDa (upper) complex. Previous
488 deletions within ExbD periplasmic residues, 92-121, prevented ExbD from formaldehyde cross-
489 linking to ExbB (35). Therefore, it was possible that a periplasmic ExbD-ExbB interaction *could*
490 exist. However, disulfide ExbD-homodimers within this region still formaldehyde cross-linked
491 with ExbB *in vivo*. The disulfide-bonded interface would have likely prevented a potential
492 switch to a ExbB-ExbD interface and thus, it seemed unlikely that the 92-121 region directly
493 interacted with ExbB (38). But in this study, ExbD-ExbB periplasmic interactions were identified
494 throughout the ExbD disordered domain in two distinct complexes.

495 Previously, only a single ExbD-ExbB complex of ~41 kDa had been identified with
496 formaldehyde cross-linking instead of two like what was captured in this study with photo-
497 cross-linking (31). Because formaldehyde cross-linking is non-residue specific, the two ExbB-
498 ExbD complexes may be distinguished due to the multiple crosslinks within a single complex.
499 This would potentially explain why the single formaldehyde cross-linked ExbB-ExbD complex
500 is the average molecular weight of the of the two ExbB-ExbD complexes seen with photo-
501 cross-linking.

502 The ExbB-ExbD (lower) complex was captured with similar intensities from all residues
503 throughout the ExbD disordered domain (~20 residues from its TMD). Because ExbB has very
504 little of its protein exposed to the periplasm, the ExbD-ExbB (lower) complex may suggest that
505 either the N-terminal tail of ExbB (~21 amino acid from its 1st TMD) is extended into the
506 periplasm or that the ExbD disordered domain is parallel to the membrane at some point
507 during the TonB energization cycle. The latter possibility would be consistent with one of the
508 three ExbB-ExbD structures isolated and mapped via 3D electron microscopy with ratios 4:2 in
509 which electron density of the ExbD periplasmic domain parallel with the membrane (58). It
510 would also be consistent with what was seen in the ExbD homolog, TolR of Tol system, in
511 which its C-terminus interacts with the ExbB homolog, TolQ (59). However, these correlations
512 would need to be further examined *in vivo* to determine if they are related observations.

513 The ExbD-ExbB (upper) complex was captured most strongly from residues
514 immediately distal to ExbD TMD and significantly waned after the first six N-terminal residues
515 of the ExbD disordered domain. Considering the presumed location of these residues, it seems
516 plausible that the ExbB-ExbD (upper) complex may be from where the initial periplasmic
517 residues of ExbD interacts with ExbB as it extends into the periplasm. This logic would
518 potentially explain why only ExbD residues nearest to its TMD captured this complex. The
519 ExbB-ExbD (upper) complex also may be suggestive of an ExbD extended conformation as
520 seen in a second ExbB-ExbD structure isolated and mapped via 3D electron microscopy (58).
521 However due to the lack of resolution, the ExbD disordered domain in the isolated ExbB-ExbD
522 structure from 3D electron microscopy could not be identified.

523 The addition of CCCP did not prevent ExbD disordered residues from the ExbB-ExbD
524 (upper) or ExbB-ExbD (lower) photo-cross-linked complexes. Therefore, neither ExbB-ExbD
525 complex was dependent of PMF. In a previous finding, the degree of Oregon Green® 488

526 maleimide labelling of cytoplasmic tail mutant TonB (L3C) was dependent its interactions with
527 the TBDTs. Because ExbB is presumably the only TonB system protein with large portion of its
528 protein in the cytoplasm, conformational changes within ExbB may influence the maleimide
529 labelling of the TonB cytoplasmic tail (60). Perhaps, the two photo-cross-linked ExbD-ExbB
530 complexes in this work are related to ExbB conformational changes that influence the Oregon
531 Green® 488 maleimide labelling of cytoplasmic tail mutant TonB (L3C). Further analysis would
532 be needed to determine if either ExbB-ExbD complex is influenced by the TonB-TBDT
533 interactions.

534 *ExbD-ExbD complexes* - The ExbD homodimer (~31 kDa) was also identified via *in vivo*
535 photo-cross-linking and had a similar molecular weight to the formaldehyde-cross-linked ExbD
536 homodimer (~30 kDa) (31). Except for ExbD (P50pBpa) or ExbD (A51pBpa), the intensity of
537 the ExbD homodimer complex gradually decreased with residues more distant from the TMD.
538 Because the residues that capture ExbD homodimers are immediately distal to its TMD, it
539 seems likely that the ExbD TMDs would be in close proximity. However this is not suggested in
540 a recent crystal structure (61).

541 Most of the ExbD disordered residues that captured ExbD homodimers did not capture
542 the PMF-dependent ExbD-TonB heterodimers. This indicates that most residues within its
543 disordered domain that have ExbD homodimeric interfaces do not share one with a PMF-
544 dependent ExbD-TonB interaction, which would differ from a mostly shared interface identified
545 within the ExbD 92-121 region (38). This suggests that transition from an ExbD homodimer to
546 PMF-dependent ExbD-TonB swap may be region specific. Similarly, TonB homodimers remain
547 active throughout the transduction cycle when they are tethered close to its TMD, but they are
548 inactive as a homodimer when they are tethered at the C-terminus, presumably because it
549 prevented the TonB C-terminus to form other necessary interactions (26). The observations in

550 this work may support the idea that the TonB system protein partner transition is instead likely
551 partner interface transitions that can occur different steps throughout the TonB energization
552 cycle.

553 It is mostly unclear about what enables the transition between the captured photo-cross-
554 linked ExbD complexes, many from which were captured by a single residue. Other than the
555 PMF-dependent ExbD-TonB interaction, none of the ExbD complexes were dependent on
556 PMF. Perhaps the complex transitions are influenced from ExbB, or a hypothesized mystery
557 protein(s) of the system (16, 42, 60). ExbB also has a predicted disordered region within its
558 cytoplasmic loop (16) in which deletions within the region cause growth arrest (42). It would be
559 interesting if ExbB has any role in dictating any of the disordered domain ExbD interaction
560 transitions or if signaling comes from the TBDT or from ligand-TBDT interaction.

561 **The *in vivo* data as it relates to recent structures**
562
563 Historically, purified structures within the TonB system have been controversial., The
564 ratio of the components of isolated TonB system complexes have not been internally
565 consistent [i.e. 4ExbB: 2ExbD and 4ExbB: 1ExbD: 1TonB from single particle EM studies (58,
566 48); 5ExbB:1ExbD and 6ExbB:3ExbD from crystal structure determinations (61, 62);
567 6ExbB:1ExbD from mass spectrometry (63); and most recently, 5ExbB: 2ExbD from cryo-EM
568 (64)], nor consistent with the system's *in vivo* cellular ratio of 7ExbB: 2ExbD: 1TonB (17).

569 Recently, two crystal structures and a cryo-EM structure have been published: 5 ExbB
570 with 1 ExbD TMD in the pore (crystal); 6 ExbB: 3 ExbD TMD in the pore (crystal); 5 ExbB: 2
571 ExbD TMD in the pore (cryo-EM) (61, 62, 64). While the ExbB monomers within the structures
572 make sense based on what is known about ExbB, the oligomeric structures diverge from what
573 is known *in vivo* about ExbB oligomers. 1) ExbB forms formaldehyde- cross-linked tetramers
574 as a dimer of homodimers *in vivo* and cross-links strongly to TonB (30). To date, TonB is

575 absent from all structures, but a single particle electron microscopy (EM) study, where it was
576 present in a complex of 4ExbB:1ExbD:1TonB (48). Consistent with that, our *in vivo* photo-
577 cross-linking data from this study indicated that ExbD (I24pBpa) in the ExbD TMD, captured
578 the ExbD-TonB PMF-independent complex, likely through direct interaction with the TonB
579 TMD. 2) Neither crystal nor the cryo-EM structure of ExbB oligomers permits ExbD and TonB
580 to interact through their transmembrane domains because the lumens of the ExbB pentamers
581 or hexamers are fully occupied by ExbD TMDs. Thus, TonB is proposed to bind on the
582 perimeter of the ExbB pentamer or hexamer (61, 62). 3) The TonB TMD interacts with ExbB
583 TMD1 *in vivo* (16), however, it is clear that TonB moves through its energization cycle stably
584 homodimerized near and probably through its TMD (26). While TMD1 is indeed on the outside
585 of the pentamer/hexamer structures, it is not possible to arrange TonB TMDs outside the ExbB
586 pentamer/hexamer TMDs such that two TonB TMDs can dimerize. 4) Since TonB moves
587 through its energy transduction cycle homodimerized through its N-terminus (26). TonB on the
588 periphery of ExbB oligomers results in a ratio of 5-6 ExbB:10-12 TonB, which conflicts with the
589 known cellular ratio of 7ExbB: 1TonB (17). One way to accommodate TonB homodimers on
590 the outside and at the known cellular ratios, is for one of the crystal structure subunits to
591 display asymmetry, such that it differed from the other members of the oligomer and could be
592 the only one to bind TonB. However, this was not observed.

593 It is well-established that TolR and MotB, paralogues of ExbD, form functional
594 homodimers *in vivo* (65, 66). In our study, several functionally active ExbD amber substitutions
595 immediately distal to the N-terminal ExbD TMD captured ExbD homodimers (but not
596 homotrimers). In addition, ExbD (I24pBpa) in the ExbD TMD, which is admittedly inactive, also
597 captured ExbD homodimers but not homotrimers. These data are contrary to the pentameric
598 ExbB crystal structure with only one ExbD TMD within its lumen and the hexameric ExbB

599 crystal structure with three ExbD TMDs within its lumen (61, 62). If ExbD homotrimers exist *in*
600 *vivo*, they must be asymmetrically arranged within the ExbB hexamer, and still without space
601 to accommodate contact with the TonB TMD (62). Although the cryo-EM structure had two
602 ExbD TMDs within its lumen, it also did not have space to accommodate the TonB TMD (64).

603 The discrepancies between *in vivo* results and *in vitro* ExbB structures raise questions
604 about the role they play in TonB-dependent energy transduction. Our current model suggests
605 stages in that process, and in this study, we identified important contacts among ExbD, TonB
606 and ExbB that occurred during those stages. Perhaps the *in vitro* structures represent as-yet-
607 unidentified intermediates. Nonetheless the absence of TonB from the ExbB *in vitro* structures,
608 and the skewed ratios that result when, as the crystal structure papers propose, TonB
609 homodimers are arranged on the peripheries of the ExbB oligomers, raise questions that need
610 to be resolved.

611 **The functional role of ΨXΨXLP motif within the ExbD disordered domain**

612 The most important function within ExbD disordered domain is the essential ΨXΨXLP
613 motif. Double-alanine mutations within this motif were completely inactive of nearly all TonB
614 system activity and stalled the TonB energization cycle in Stage II. The parallels with the
615 ΨXΨXLP motif and the PMF-unresponsive ExbD mutant, ExbD (D25N), suggest that the motif
616 is required for ExbD to respond to PMF. Supporting this idea, ExbD pBpa substitutions with
617 V45A and V47A substitutions, prevented ExbD (S54pBpa) and ExbD (K97pBpa) from forming
618 the PMF-dependent ExbD-TonB interaction. However, due to the inactivity of the pBpa
619 substitutions within this motif, it is difficult to determine if these residues are directly or
620 indirectly involved in the ExbD-TonB PMF-dependent interaction.

621 The V45A, V47A mutations also caused additional unknown ExbD complex formations.
622 Although these complexes are unidentified, it demonstrates that the ΨXΨXLP motif influences

623 distant ExbD C-terminal residue interactions. The motif may be important for conformational
624 changes in ExbD C-terminus to form the correct interactions and potentially highlights a
625 protein-wide functional role of the ΨXΨXLP motif in signal transduction.

626 The ExbD ΨXΨXLP motif is also conserved its paralog, TolR, but not in a more distant
627 paralog, MotB of the flagellar MotAB energy harvesting complex. Unlike MotAB, TolQR and
628 ExbBD complexes can account for detectable levels of TonB system and the Tol system
629 activity respectively (23, 43). However, the molecular mechanism of how these systems cross-
630 talk is unclear. Because the motif is important for the TonB system to response to PMF, it
631 seems likely this motif would be important for the Tol system to respond to PMF. Perhaps, the
632 conserved motif among both TolR and ExbD may provide molecular insight to how the
633 complexes cross-talk. It would be interesting if mutations in TolR ΨXΨXLP motif also are
634 important C-terminal interactions. Maybe the motif and its function are conserved in both ExbD
635 and TolR but, it triggers different system-specific C-terminal conformational changes.
636 Nonetheless, the role the ΨXΨXLP motif as it functions in TolR will need to be examined to
637 verify to the functional similarities.

638 **Similarities and differences between the ExbD homodimers and the homolog, TolR,**
639 **dimeric crystal structure**

640 The ExbB, ExbD, and TonB are homologous TolQ, TolR, and TolA of the outer-
641 membrane integrity complex called the Tol system (43, 50). The homology among each
642 corresponding protein occurs mostly through their TMDs, however, the ExbD periplasmic
643 disordered domain ΨXΨXLP motif is also conserved in TolR. Although ExbBD and TolQR
644 have functional cross-talk, TonB and TolA do not. This an important divergence of function of
645 each system. But considering that the ΨXΨXLP motif is conserved in both ExbD and TolR, it is
646 reasonable that the motif function is also conserved. In the ExbD NMR structure, ΨXΨXLP

647 motif exists as part of the ExbD disordered domain, however, a dimeric crystal structure of
648 TolR, periplasmic domains shows that a portion of the ΨXΨXLP motif in a beta strand (67).
649 The structure had a homodimeric interface that included residues 41, 43-47, 49 which
650 corresponded with the ExbD disordered domain residues 43,45-49, and 51 (Fig. S4). Our work
651 shows that ExbD homodimers were most abundant through residues 45-49 and 52-55
652 (residues 43-47 and 50-53 in TolR), which would be somewhat consistent with a similar
653 dimeric interface in ExbD as in the TolR structure. However, there were some differences
654 between the two interfaces. TolR (D49) was the final residue at its structural dimeric interface
655 but the ExbD position equivalent (A51) captured very little ExbD homodimer. Moreover, four
656 ExbD residues after A51 – S52, T53, S54, and T55 (TolR D49 - A50, T51, E52, and S53) –
657 captured significant amounts of homodimers, but were implicated as such in the TolR dimeric
658 structure (67). The conservation between TolR and ExbD wanes after a conserved proline
659 [ExbD (P50) and TolR (P48)] of the ΨXΨXLP motif until the final ~35 residues of ExbD (68).
660 Considering the difference between the physical properties of an aspartate and an alanine,
661 instead of ExbD A51, ExbD polar residues 52-55 may be the ExbD functionally equivalent to
662 TolR residue D49.

663 Although a similar dimeric interface as the TolR crystal structure may exist in ExbD, our
664 data support the Wojdyla et al. conclusions that this structure in ExbD cannot remain static *in*
665 *vivo* (67). Using the photo-cross-linking approach, a single residue could trap all contacts
666 throughout its transition of the TonB energization cycle which better demonstrates the dynamic
667 behavior ExbD and its signal transduction. We have identified multiple interacting partners with
668 single ExbD residues within the ExbD disordered domain. This indicates that the ExbD
669 disordered domain needs to interact with different partners as it proceeds through the TonB
670 energization cycle and therefore, it cannot remain static in a dimeric conformation.

671 **Proposed function of the motif as it pertains to the Stages during the TonB energization**
672 **cycle**

673 The ΨXΨXLP motif is required to transition from Stage II to Stage III of the TonB
674 energization cycle. Alanine mutations for the branched hydrophobic residues in the ΨXΨXLP
675 motif are still able to convert TonB into a conformation that produces the TonB proteinase K-
676 resistant fragment indicative of Stage II. Therefore, the hydrophobic-branched residues are not
677 needed for initial association with TonB. The ExbD (S54pBpa) photo-cross-linked ExbD-TonB
678 PMF-independent interaction is unaffected with the V45A and V47A mutations, yet distal ExbD
679 pBpa substitutions, K97 and E136, with the mutations had reduced TonB interactions. This
680 may suggest that TonB is initially recognized by residues within the disordered domain before
681 the function of the motif is required. Perhaps, the initial association with TonB is what signals
682 to the system to assume Stage II. And at this point, the ExbD disordered domain interacts with
683 TonB in a way that either directly protects ~155 residues of TonB or influences TonB to
684 assume Proteinase K, resistant conformation. Then, through an unclear mechanism, the ExbD
685 ΨXΨXLP motif is required to transition the PMF-independent ExbD-TonB interaction in Stage
686 II to a PMF-dependent ExbD-TonB interaction in Stage III.

687 **Summary:**

688 The data show that the ExbD disordered domain is a highly dynamic region and is
689 involved in many system protein-protein interactions. The function of this domain is a
690 highlighted by the ΨXΨXLP motif that is essential for TonB system activity and the ExbD-TonB
691 PMF-dependent interaction. Because the ExbD disordered domain interacted with several
692 partners and contains an essential motif for TonB activity, this would a promising target for a
693 novel antibiotic against the TonB system in *Escherichia coli* and Gram-negative pathogens.
694

695

696

697 **MATERIALS and METHODS:**

698 **Strains and plasmids.** Strains and plasmids used in these studies are listed in Table S1.
699 Strain KP1526 was constructed by P1*vir transduction of* Δ*exbD::cam in RA1021 (W3110,*
700 Δ*exbD::cam) into RA1525 (W3110,* Δ*tolQR,* Δ*aroB*) [(35)*, RA1021 and RA1525* were kind gifts
701 from Ray Larsen]. The *tolQR* genes were deleted to eliminate crosstalk (43). Plasmids with
702 encoded alanine and amber substitution mutations were mostly derived from pKP999.Amber
703 substitutions in ExbD (V45A, V47A) encoding plasmids were derived from pKP2171. To
704 determine the identity of potential ExbB complexes, we added a His6X epitope tag to the C-
705 terminus of ExbB in the vector pKP1657 which carries the ExbBD operon and re-engineered
706 the ExbD pBpa substitutions on that plasmid. Plasmids pKP2159 and pKP2160 were derived
707 from pKP2145 and pKP2154, respectively. All plasmids were made using 25-cycle extralong
708 PCR. 5'-phosphorylated primers were used with the desired mutation encoded in the forward
709 primer and are available upon request. All mutants were verified by DNA sequencing at the
710 Penn State Genomics Core Facility, University Park, PA.

711 **Media and growth conditions.** All cultures were grown at 37˚C with aeration. Saturated
712 cultures in Luria-Bertani broth were subcultured at 1:75 in M9 minimal media supplemented
713 with 0.4% glycerol, 0.2% Casamino Acids, 40 µg/ml tryptophan, 4 µg/ml vitamin B1, 1 mM
714 $MgSO_4$, 0.5 mM $CaCl_2$, and 37 µM $FeCl_3$. All cultures carrying plasmids with *exbD* were in
715 RA1045 (W3110, Δ*exbD*, Δ*tolQR*) unless noted and grown in 100 µg/mL ampicillin.
716 Subcultures were induced with sodium propionate (ranging from 0-45 mM) to approximate the
717 steady state levels of ExbD protein from W3110, the wildtype control (Table S1). All
718 subcultures were harvested at an A_{550} ranging from 0.40 to 0.60.

719 ***In vivo* formaldehyde-cross-linking**. Culture conditions were as described above. Culture
720 volumes were adjusted to harvest 0.5 A_{550} -mL of cells. Bacteria were resuspended in sodium
721 phosphate buffer (pH 6.8) and treated for 15 min at room temperature with 1% formaldehyde
722 (Electron Microscopy Sciences Cat #15710) as previously described (69). Following
723 formaldehyde treatment, bacteria were suspended in Laemmli sample buffer (70), with equal
724 cell numbers loaded in each well of 13% sodium dodecyl sulfate (SDS)-polyacrylamide gels.
725 ExbD complexes and TonB complexes were detected by immunoblotting with ExbD-specific
726 polyclonal antibodies and TonB-specific monoclonal antibodies, respectively (14, 71). Equal
727 loads were confirmed by Coomassie staining of the PVDF membrane used for the immunoblot.

728 ***In vivo* photo-cross-linking.** For *in vivo* photo-cross-linking, plasmids with amber
729 substitutions in *exbD* were co-expressed with pEVOL in RA1045 (W3110, Δ*exbD*, Δ*tolQR*),
730 which encodes an orthogonal tRNA synthetase and the corresponding orthogonal $tRNA_{CUA}$
731 that recognizes amber (UAG) codons (72). Cultures were grown to saturation in 100 µg/mL
732 ampicillin and 34 µg/mL chloramphenicol. Subcultures were grown in minimal M9 medium as
733 described above. At A_{550} of ~0.2, subcultures were treated with 0.004**%** arabinose (tRNA
734 synthetase/tRNA pair induction from pEVOL; Table S1), 0.8 mM the photo-cross-linkable
735 amino acid p-Benzoyl-L-phenylalanine (pBpa) and amounts of propionate required for ExbD
736 protein expression at near-chromosomal levels (Table S1). 2.0 A_{550}-ml were harvested at A_{550}
737 ~ 0.5, pelleted at room temperature and resuspended in 2 mL supplemented M9 media (as
738 described above with 1.85 µM $FeCl_3$ and without antibiotics, pBpa, and propionate). Equal
739 volumes of each sample were transferred into single wells of each of two 24-well plates (NEST
740 Cell Culture Plate, cat: 702001). One plate was irradiated with 365-nm light for 30 min at room
741 temperature and the second plate was incubated in the dark simultaneously for 30 min at room
742 temperature. Samples were precipitated with 10% trichloroacetic acid (TCA) as described

743 previously and processed for immunoblot analysis with ExbD-specific polyclonal antibodies
744 and TonB-specific monoclonal antibodies (14, 71). Equal loads were confirmed by Coomassie
745 staining of the PVDF membrane used for the immunoblot.

746 **Initial rates of ^{55}Fe-ferrichrome and ^{55}Fe-enterochelin transport**. Cultures were grown as
747 described in media and growth conditions. Strains harboring plasmids with and without amber
748 substitutions in *exbD* were grown as described in the *in vivo* photo- cross-linking section. ^{55}Fe-
749 ferrichrome assay and ^{55}Fe-ferrichrome assay were performed in triplicate as previously
750 described (40). To exclude competition from native enterochelin, ^{55}Fe-enterochelin uptake was
751 assessed in *aroB*- strains that were subcultured with additional phenylalanine (40 µg/ml) and
752 tyrosine (40 µg/ml) to compensate for their inability to synthesize aromatic amino acids. To
753 determine steady state levels of the different ExbD variants, samples were precipitated with
754 10% TCA at the start of the assay and equivalent numbers of cells processed for immunoblot
755 analysis on 13% SDS-polyacrylamide gels. ExbD proteins were detected by immunoblotting
756 with ExbD-specific polyclonal antibodies (14, 71).

757 **Ethidium bromide accumulation.** Sub-cultures were grown as described above. At A_{550} of
758 0.5, 2 mL of cells were transferred to 4.5 mL disposable cuvettes (VWR Cat# 30620-276)
759 Ethidium bromide (6.25 µM) was added to the cells and fluorescence was detected using a LS-
760 55 fluorescence spectrophotometer. The excitation wavelength was 520 nm and the emission
761 wavelength was 590 nm. The width of the excitation and emission slits were 15 nm.
762 Fluorescence emission data was collected every second for 3 minutes using the Time Drive
763 application from the FLWINLAB software. For CCCP controls, either 15 µM or 60 µM CCCP
764 was added two minutes prior to ethidium bromide. The ethidium bromide accumulation rate for
765 each sample was determined by linear regression and recorded as Fluorescence Units per
766 second (FU/sec).

767 **Proteinase K Accessibility**. TonB sensitivity to proteinase K was performed as previously
768 described (8, 16, 35) Cultures were grown as described in media and growth conditions.
769 Spheroplasts were made as previously described (8). Samples were treated with carbonyl
770 cyanide *m*-chlorophenylhydrazone (60 μM), CCCP, where indicated 5 min prior to proteinase K
771 treatment (25 μg/mL). Samples were collected at 2 min, 5 min, 10 min, and 15 min following
772 proteinase K treatment with the addition of phenylmethylsulfonyl fluoride (1.0 mM) to inactivate
773 proteinase K at the specified times. Samples were precipitated with 10% TCA final
774 concentration and suspended in Laemmli sample buffer (70). Samples were loaded with equal
775 volumes on 13% SDS-polyacrylamide gels. Were detected via immunoblotting with ExbD-
776 specific polyclonal antibodies and TonB-specific monoclonal antibodies (14, 71).

777 **Multiple Sequence Alignment.** A sequence logo of the ExbD disordered region was
778 generated from a multiple sequence alignment by using HHblits in the Gremelin.bakerlab
779 program (73). Sequences aligned were all within an expect score of e^{-10} of *Escherichia coli K-*
780 *12 strain* (NP_417478.1). Positions were removed with >75% sequences alignment gaps. The
781 sequence for *Escherichia coli* ExbD (AAA69172.1), TolR (PSM33938.1), and MotB
782 (ACB03086.1) were aligned using clustal multiple sequence alignment generated by MUSCLE
783 (3.8).

784 **Colicin Sensitivity Assay.** The colicin sensitivity assay was performed as previously
785 described (40). Strains were grown to mid-exponential phase with expressing ExbD in T-broth.
786 The expression was confirmed by precipitation of cultures with trichloroacetic acid (TCA) and
787 were detected by immunoblot comparison to W3110. Cells were plated in T-top agar on T-
788 plates containing equal propionate concentrations as was in the sub-culture with 100 μg/ml
789 ampicillin. Five-fold dilutions of Colicins B, Ia, or M (Colicin B enters via FepA; Colicin Ia enters
790 via CirA; Colicin M enters FhuA) were spotted on the bacterial lawns and were incubated

791 overnight at 37°C. Scoring was reported as the highest dilution that produced clearing. The
792 assay was done in triplicate.

793

794 **ACKNOWLEDGEMENTS:**

795 Support from NIAID for grant AI11322 to K.P. is gratefully acknowledged.

796 **REFERENCES:**

797 1. Schauer K, Rodionov DA, Reuse H de. 2008. New substrates for TonB-dependent
798 transport: do we only see the 'tip of the iceberg'? Trends in Biochemical Sciences 33:330–
799 338.

800 2. Sheldon JR, Laakso HA, Heinrichs DE. 2016. Iron Acquisition Strategies of Bacterial
801 Pathogens. Microbiology Spectrum 4.

802 3. Miethke M, Marahiel MA. 2007. Siderophore-Based Iron Acquisition and Pathogen
803 Control. Microbiol Mol Biol Rev 71:413–451.

804 4. Noinaj N, Guillier M, Barnard TJ, Buchanan SK. 2010. TonB-dependent transporters:
805 regulation, structure, and function. Annu Rev Microbiol 64:43–60.

806 5. Hickman SJ, Cooper REM, Bellucci L, Paci E, Brockwell DJ. 2017. Gating of TonB-
807 dependent transporters by substrate-specific forced remodelling. Nature Communications
808 8:14804.

809 6. Gresock MG, Postle K. 2017. Going Outside the TonB Box: Identification of Novel FepA-
810 TonB Interactions In Vivo. J Bacteriol 199.

811 7. Ferguson AD, Amezcua CA, Halabi NM, Chelliah Y, Rosen MK, Ranganathan R,
812 Deisenhofer J. 2007. Signal transduction pathway of TonB-dependent transporters. PNAS
813 104:513–518.

814 8. Larsen RA, Thomas MG, Postle K. 1999. Protonmotive force, ExbB and ligand-bound
815 FepA drive conformational changes in TonB. Molecular Microbiology 31:1809–1824.

816 9. Moeck GS, Coulton JW, Postle K. 1997. Cell envelope signaling in Escherichia coli.
817 Ligand binding to the ferrichrome-iron receptor fhua promotes interaction with the energy-
818 transducing protein TonB. J Biol Chem 272:28391–28397.

819 10. Cornelissen CN, Anderson JE, Sparling PF. 1997. Energy-dependent changes in the
820 gonococcal transferrin receptor. Mol Microbiol 26:25–35.

821 11. Khursigara CM, Crescenzo GD, Pawelek PD, Coulton JW. 2004. Enhanced Binding of
822 TonB to a Ligand-loaded Outer Membrane Receptor ROLE OF THE OLIGOMERIC
823 STATE OF TonB IN FORMATION OF A FUNCTIONAL FhuA·TonB COMPLEX. J Biol
824 Chem 279:7405–7412.

825 12. Bradbeer C. 1993. The proton motive force drives the outer membrane transport of
826 cobalamin in Escherichia coli. J Bacteriol 175:3146–3150.

827 13. Krewulak KD, Vogel HJ. 2011. TonB or not TonB: is that the question? Biochemistry &
828 Cell Biology 89:87–97.

829 14. Higgs PI, Larsen RA, Postle K. 2002. Quantification of known components of the
830 Escherichia coli TonB energy transduction system: TonB, ExbB, ExbD and FepA. Mol
831 Microbiol 44:271–281.

832 15. Kampfenkel K, Braun V. 1993. Topology of the ExbB protein in the cytoplasmic
833 membrane of Escherichia coli. J Biol Chem 268:6050–6057.

834 16. Baker KR, Postle K. 2013. Mutations in Escherichia coli ExbB Transmembrane Domains
835 Identify Scaffolding and Signal Transduction Functions and Exclude Participation in a
836 Proton Pathway. J Bacteriol 195:2898–2911.

837 17. Roof SK, Allard JD, Bertrand KP, Postle K. 1991. Analysis of Escherichia coli TonB
838 membrane topology by use of PhoA fusions. Journal of Bacteriology 173:5554–5557.

839 18. Kampfenkel K, Braun V. 1992. Membrane topology of the Escherichia coli ExbD protein.
840 Journal of Bacteriology 174:5485–5487.

841 19. Bernadac A, Gavioli M, Lazzaroni J-C, Raina S, Lloubès R. 1998. Escherichia coli tol-pal
842 Mutants Form Outer Membrane Vesicles. J Bacteriol 180:4872–4878.

843 20. Masilamani R, Cian MB, Dalebroux ZD. 2018. Salmonella Tol-Pal Reduces Outer
844 Membrane Glycerophospholipid Levels for Envelope Homeostasis and Survival during
845 Bacteremia. Infect Immun 86.

846 21. Gerding MA, Ogata Y, Pecora ND, Niki H, de Boer PAJ. 2007. The trans-envelope Tol-Pal
847 complex is part of the cell division machinery and required for proper outer-membrane
848 invagination during cell constriction in E. coli. Mol Microbiol 63:1008–1025.

849 22. Cascales E, Lloubès R, Sturgis JN. 2001. The TolQ-TolR proteins energize TolA and
850 share homologies with the flagellar motor proteins MotA-MotB. Mol Microbiol 42:795–807.

851 23. Brinkman KK, Larsen RA. 2008. Interactions of the Energy Transducer TonB with
852 Noncognate Energy-Harvesting Complexes. J Bacteriol 190:421–427.

853 24. Kadner RJ, Heller KJ. 1995. Mutual inhibition of cobalamin and siderophore uptake
854 systems suggests their competition for TonB function. J Bacteriol 177:4829–4835.

855 25. Kaserer WA, Jiang X, Xiao Q, Scott DC, Bauler M, Copeland D, Newton SMC, Klebba PE.
856 2008. Insight from TonB hybrid proteins into the mechanism of iron transport through the
857 outer membrane. J Bacteriol 190:4001–4016.

858 26. Gresock MG, Kastead KA, Postle K. 2015. From Homodimer to Heterodimer and Back:
859 Elucidating the TonB Energy Transduction Cycle. Journal of Bacteriology 197:3433–3445.

860 27. Chang C, Mooser A, Plückthun A, Wlodawer A. 2001. Crystal structure of the dimeric C-
861 terminal domain of TonB reveals a novel fold. J Biol Chem 276:27535–27540.

862 28. Pawelek PD, Croteau N, Ng-Thow-Hing C, Khursigara CM, Moiseeva N, Allaire M,
863 Coulton JW. 2006. Structure of TonB in Complex with FhuA, E. coli Outer Membrane
864 Receptor. Science 312:1399–1402.

865 29. Ghosh J, Postle K. 2004. Evidence for dynamic clustering of carboxy-terminal aromatic
866 amino acids in TonB-dependent energy transduction. Mol Microbiol 51:203–213.

867 30. Jana B, Manning M, Postle K. 2011. Mutations in the ExbB cytoplasmic carboxy terminus
868 prevent energy-dependent interaction between the TonB and ExbD periplasmic domains.
869 J Bacteriol 193:5649–5657.

870 31. Ollis AA, Manning M, Held KG, Postle K. 2009. Cytoplasmic Membrane Protonmotive
871 Force Energizes Periplasmic Interactions between ExbD and TonB. Mol Microbiol
872 73:466–481.

873 32. Skare JT, Postle K. 1991. Evidence for a TonB-dependent energy transduction complex in
874 Escherichia coli. Mol Microbiol 5:2883–2890.

875 33. Fischer E, Günter K, Braun V. 1989. Involvement of ExbB and TonB in transport across
876 the outer membrane of Escherichia coli: phenotypic complementation of exb mutants by
877 overexpressed tonB and physical stabilization of TonB by ExbB. J Bacteriol 171:5127–
878 5134.

879 34. Ollis AA, Postle K. 2012. ExbD mutants define initial stages in TonB energization. J Mol
880 Biol 415:237–247.

881 35. Ollis AA, Kumar A, Postle K. 2012. The ExbD Periplasmic Domain Contains Distinct
882 Functional Regions for Two Stages in TonB Energization. Journal of Bacteriology
883 194:3069–3077.

884 36. Swayne C, Postle K. 2011. Taking the Escherichia coli TonB Transmembrane Domain
885 “Offline”? Nonprotonatable Asn Substitutes Fully for TonB His20. Journal of Bacteriology
886 193:3693–3701.

887 37. Garcia-Herrero A, Peacock RS, Howard SP, Vogel HJ. 2007. The solution structure of the
888 periplasmic domain of the TonB system ExbD protein reveals an unexpected structural
889 homology with siderophore-binding proteins. Mol Microbiol 66:872–889.

890 38. Ollis AA, Postle K. 2011. The Same Periplasmic ExbD Residues Mediate In Vivo
891 Interactions between ExbD Homodimers and ExbD-TonB Heterodimers ▿. J Bacteriol
892 193:6852–6863.

893 39. Ollis AA, Postle K. 2012. Identification of Functionally Important TonB-ExbD Periplasmic
894 Domain Interactions In Vivo. Journal of Bacteriology 194:3078–3087.

895 40. Postle K. 2007. [12] - TonB System, In Vivo Assays and Characterization, p. 245–269. *In*
896 Simon, MI, Crane, BR, Crane, A (eds.), Methods in Enzymology. Academic Press.

897 41. Takatsuka Y, Nikaido H. 2009. Covalently Linked Trimer of the AcrB Multidrug Efflux
898 Pump Provides Support for the Functional Rotating Mechanism. J Bacteriol 191:1729–
899 1737.

900 42. Bulathsinghala CM, Jana B, Baker KR, Postle K. 2013. ExbB Cytoplasmic Loop Deletions
901 Cause Immediate, Proton Motive Force-Independent Growth Arrest. J Bacteriol
902 195:4580–4591.

903 43. Braun V, Herrmann C. 1993. Evolutionary relationship of uptake systems for biopolymers
904 in Escherichia coli: cross-complementation between the TonB-ExbB-ExbD and the TolA-
905 TolQ-TolR proteins. Mol Microbiol 8:261–268.

906 44. Ryu Y, Schultz PG. 2006. Efficient incorporation of unnatural amino acids into proteins in
907 Escherichia coli. Nat Methods 3:263–265.

908 45. Braun V, Gaisser S, Herrmann C, Kampfenkel K, Killmann H, Traub I. 1996. Energy-
909 coupled transport across the outer membrane of Escherichia coli: ExbB binds ExbD and
910 TonB in vitro, and leucine 132 in the periplasmic region and aspartate 25 in the
911 transmembrane region are important for ExbD activity. Journal of Bacteriology 178:2836–
912 2845.

913 46. Dormán G, Prestwich GD. 1994. Benzophenone photophores in biochemistry.
914 Biochemistry 33:5661–5673.

915 47. Metz B, Kersten GFA, Hoogerhout P, Brugghe HF, Timmermans HAM, Jong A de,
916 Meiring H, Hove J ten, Hennink WE, Crommelin DJA, Jiskoot W. 2004. Identification of
917 Formaldehyde-induced Modifications in Proteins REACTIONS WITH MODEL PEPTIDES.
918 J Biol Chem 279:6235–6243.

919 48. Sverzhinsky A, Chung JW, Deme JC, Fabre L, Levey KT, Plesa M, Carter DM,
920 Lypaczewski P, Coulton JW. 2015. Membrane Protein Complex ExbB4-ExbD1-TonB1
921 from Escherichia coli Demonstrates Conformational Plasticity. J Bacteriol 197:1873–1885.

922 49. Brinkman KK, Larsen RA. 2008. Interactions of the Energy Transducer TonB with
923 Noncognate Energy-Harvesting Complexes. Journal of Bacteriology 190:421–427.

924 50. Braun V. 1989. The structurally related exbB and tolQ genes are interchangeable in
925 conferring tonB-dependent colicin, bacteriophage, and albomycin sensitivity. Journal of
926 Bacteriology 171:6387–6390.

927 51. Larsen RA, Chen GJ, Postle K. 2003. Performance of Standard Phenotypic Assays for
928 TonB Activity, as Evaluated by Varying the Level of Functional, Wild-Type TonB. Journal
929 of Bacteriology 185:4699–4706.

930 52. Cascales E, Buchanan SK, Duché D, Kleanthous C, Lloubès R, Postle K, Riley M, Slatin
931 S, Cavard D. 2007. Colicin biology. Microbiol Mol Biol Rev 71:158–229.

932 53. van der Lee R, Buljan M, Lang B, Weatheritt RJ, Daughdrill GW, Dunker AK, Fuxreiter M,
933 Gough J, Gsponer J, Jones DT, Kim PM, Kriwacki RW, Oldfield CJ, Pappu RV, Tompa P,
934 Uversky VN, Wright PE, Babu MM. 2014. Classification of Intrinsically Disordered Regions
935 and Proteins. Chem Rev 114:6589–6631.

936 54. Jiang J, Zhang X, Chen Y, Wu Y, Zhou ZH, Chang Z, Sui S-F. 2008. Activation of DegP
937 chaperone-protease via formation of large cage-like oligomers upon binding to substrate
938 proteins. PNAS 105:11939–11944.

939 55. Krojer T, Sawa J, Schäfer E, Saibil HR, Ehrmann M, Clausen T. 2008. Structural basis for
940 the regulated protease and chaperone function of DegP. Nature 453:885–890.

941 56. Larsen RA, Deckert GE, Kastead KA, Devanathan S, Keller KL, Postle K. 2007. His20
942 Provides the Sole Functionally Significant Side Chain in the Essential TonB
943 Transmembrane Domain. J Bacteriol 189:2825–2833.

944 57. Vakharia-Rao H, Kastead KA, Savenkova MI, Bulathsinghala CM, Postle K. 2007.
945 Deletion and Substitution Analysis of the Escherichia coli TonB Q160 Region. Journal of
946 Bacteriology 189:4662–4670.

947 58. Sverzhinsky A, Fabre L, Cottreau AL, Biot-Pelletier DMP, Khalil S, Bostina M, Rouiller I,
948 Coulton JW. 2014. Coordinated Rearrangements between Cytoplasmic and Periplasmic
949 Domains of the Membrane Protein Complex ExbB-ExbD of Escherichia coli. Structure
950 22:791–797.

951 59. Lazzaroni JC, Vianney A, Popot JL, Bénédetti H, Samatey F, Lazdunski C, Portalier R,
952 Géli V. 1995. Transmembrane α-Helix Interactions are Required for the Functional
953 Assembly of theEscherichia coliTol Complex. Journal of Molecular Biology 246:1–7.

954 60. Gresock MG, Savenkova MI, Larsen RA, Ollis AA, Postle K. 2011. Death of the TonB
955 Shuttle Hypothesis. Front Microbiol 2.

956 61. Celia H, Noinaj N, Zakharov SD, Bordignon E, Botos I, Santamaria M, Barnard TJ,
957 Cramer WA, Lloubes R, Buchanan SK. 2016. Structural insight into the role of the Ton
958 complex in energy transduction. Nature 538:60–65.

959 62. Maki-Yonekura S, Matsuoka R, Yamashita Y, Shimizu H, Tanaka M, Iwabuki F, Yonekura
960 K. 2018. Hexameric and pentameric complexes of the ExbBD energizer in the Ton
961 system. eLife 7:e35419.

962 63. Pramanik A, Hauf W, Hoffmann J, Cernescu M, Brutschy B, Braun V. 2011. Oligomeric
963 structure of ExbB and ExbB-ExbD isolated from Escherichia coli as revealed by LILBID
964 mass spectrometry. Biochemistry 50:8950–8956.

965 64. Celia H, Botos I, Ni X, Fox T, De Val N, Lloubes R, Jiang J, Buchanan SK. 2019. Cryo-EM
966 structure of the bacterial Ton motor subcomplex ExbB–ExbD provides information on
967 structure and stoichiometry. Commun Biol 2:358.

968 65. Zhang XY-Z, Goemaere EL, Thomé R, Gavioli M, Cascales E, Lloubès R. 2009. Mapping
969 the Interactions between *Escherichia coli* Tol Subunits: ROTATION OF THE TolR
970 TRANSMEMBRANE HELIX. J Biol Chem 284:4275–4282.

971 66. Braun TF, Blair DF. 2001. Targeted disulfide cross-linking of the MotB protein of
972 Escherichia coli: evidence for two H(+) channels in the stator Complex. Biochemistry
973 40:13051–13059.

974 67. Wojdyla JA, Cutts E, Kaminska R, Papadakos G, Hopper JTS, Stansfeld PJ, Staunton D,
975 Robinson CV, Kleanthous C. 2015. Structure and Function of the Escherichia coli Tol-Pal
976 Stator Protein TolR. J Biol Chem 290:26675–26687.

977 68. Eick-Helmerich K, Braun V. 1989. Import of biopolymers into Escherichia coli: nucleotide
978 sequences of the exbB and exbD genes are homologous to those of the tolQ and tolR
979 genes, respectively. J Bacteriol 171:5117–5126.

980 69. Higgs PI, Myers PS, Postle K. 1998. Interactions in the TonB-Dependent Energy
981 Transduction Complex: ExbB and ExbD Form Homomultimers. J Bacteriol 180:6031–
982 6038.

983 70. Laemmli UK. 1970. Cleavage of Structural Proteins during the Assembly of the Head of
984 Bacteriophage T4. Nature 227:680–685.

985 71. Larsen RA, Myers PS, Skare JT, Seachord CL, Darveau RP, Postle K. 1996. Identification
986 of TonB homologs in the family Enterobacteriaceae and evidence for conservation of
987 TonB-dependent energy transduction complexes. J Bacteriol 178:1363–1373.

988 72. Young TS, Ahmad I, Yin JA, Schultz PG. 2010. An Enhanced System for Unnatural Amino
989 Acid Mutagenesis in E. coli. Journal of Molecular Biology 395:361–374.

990 73. Ovchinnikov S, Kamisetty H, Baker D. 2014. Robust and accurate prediction of residue–
991 residue interactions across protein interfaces using evolutionary information. eLife 3.

992 74. Effect of loop deletions on the binding and transport of ferric enterobactin by FepA -
993 Newton - 1999 - Molecular Microbiology - Wiley Online Library.

994 75. Hill CW, Harnish BW. 1981. Inversions between ribosomal RNA genes of Escherichia coli.
995 Proc Natl Acad Sci U S A 78:7069–7072.

996
997
998
999
1000
1001
1002
1003
1004
1005
1006

FIGURES:

A.

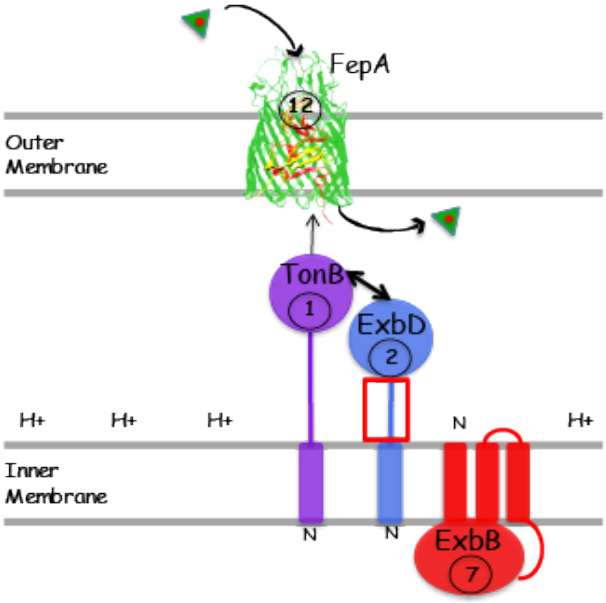

B.

Figure 1: (A) TonB-dependent energy transduction. The iron-bearing siderophore enterochelin (triangles) binds to the TBDT FepA with sub-nanomolar affinity (74). This high affinity necessitates a mechanism to release the siderophore into the periplasmic space. In the presence of cytoplasmic membrane proteins TonB, ExbB, ExbD, and the cytoplasmic membrane proton motive force (PMF), the Fe-enterochelin is actively transported across the outer membrane through FepA. Numbers indicate the ratio of the proteins in *E. coli* under iron-limiting conditions (14). Because TonB is limiting, there must be a cycle during which TonB binds and releases TBDTs. The Stages in the cycle have been studied, resulting in a model where ExbB acts as a scaffold to manage the essential interaction between TonB and ExbD that subsequently positions TonB for correct interaction with FepA. The interaction between TonB and ExbD C-termini is dependent on PMF. The red box around ExbD identifies the ExbD

1022 disordered region which is the topic of this study. Subsequent transport of enterochelin across
1023 the cytoplasmic membrane does not require the TonB system. Adapted from Gresock et al.
1024 2015, (26). (B) The NMR solution structure of ExbD periplasmic domain residues 44-141
1025 [NCBI PDB ID: 2PFU, (37)]. The alpha helices and beta strands are colored in blue and green,
1026 respectively. The ExbD disordered region is boxed in red. The first residue following the ExbD
1027 TMD, D44, and last residue, P63 of the ExbD disordered region are labeled with the side chain
1028 displayed. This image was generated using Swiss-PdbViewer [https://spdbv.vital-it.ch/(37)].

1029

1030

1031

1032

1033

1034

1035

1036

1037

1038

1039

1040

1041

1042

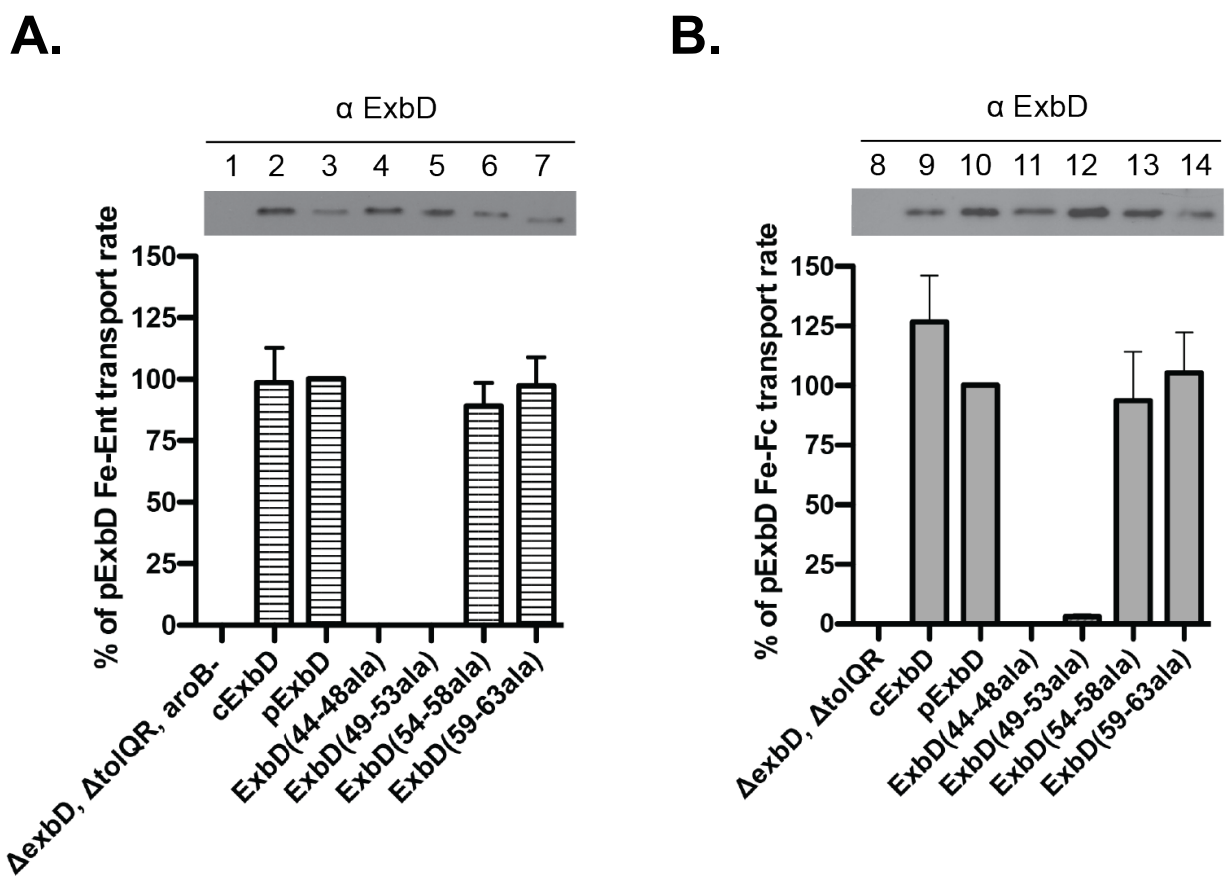

Figure 2: Block alanine substitutions of ExbD residues 44-48 and 49-53 prevent TonB system activity. (A) Initial rate of ^{55}Fe-enterochelin transport and corresponding steady-state expression levels of the ExbD proteins. Strains were grown to mid-exponential phase and assayed as described in Methods and Materials. The percentages of activity were calculated relative to the initial rate of plasmid-encoded ExbD, pExbD (pKP999), expressed at chromosomal levels in KP1526 (Δ*exbD*, Δ*tolQR, aroB-*). Assays were performed in triplicate and carried out at least twice for each strain. The slopes were determined by a linear regression fit of scintillation counts per minute. The error bars indicate mean ± SEM for a representative triplicate set (above). The steady-state ExbD monomer levels at the time of assay were determined by immunoblot analysis. To avoid competition from the only synthesized siderophore, enterochelin, in *Escherichia coli K12*, *aroB-* strains were used. cExbD designates chromosomally expressed ExbD from the wild-type strain, KP1270 (W3110,

1057 *aroB*-). ExbD alanine substitution mutants are expressed from plasmids in KP1526 (Δ*exbD*,
1058 Δ*tolQR, aroB*-). (B) Initial rate of ^{55}Fe-ferrichrome transport and corresponding steady-state
1059 expression levels of ExbD proteins. The assay was performed and analyzed identically as in
1060 (A) with using the siderophore, ferrichrome, which is transported through the TonB-dependent
1061 transporter, FhuA. The percentages of activity were calculated relative to the initial rate of
1062 plasmid-encoded ExbD, pExbD (pKP999) expressed at chromosomal levels in RA1045
1063 (Δ*exbD*, Δ*tolQR*). cExbD designates chromosomally expressed ExbD from the wild-type strain,
1064 W3110. All ExbD alanine substitution mutants are expressed from plasmids in RA1045
1065 (Δ*exbD*, Δ*tolQR*). The plasmid identities and concentrations of propionate for chromosomal
1066 expression are listed in Table S1.

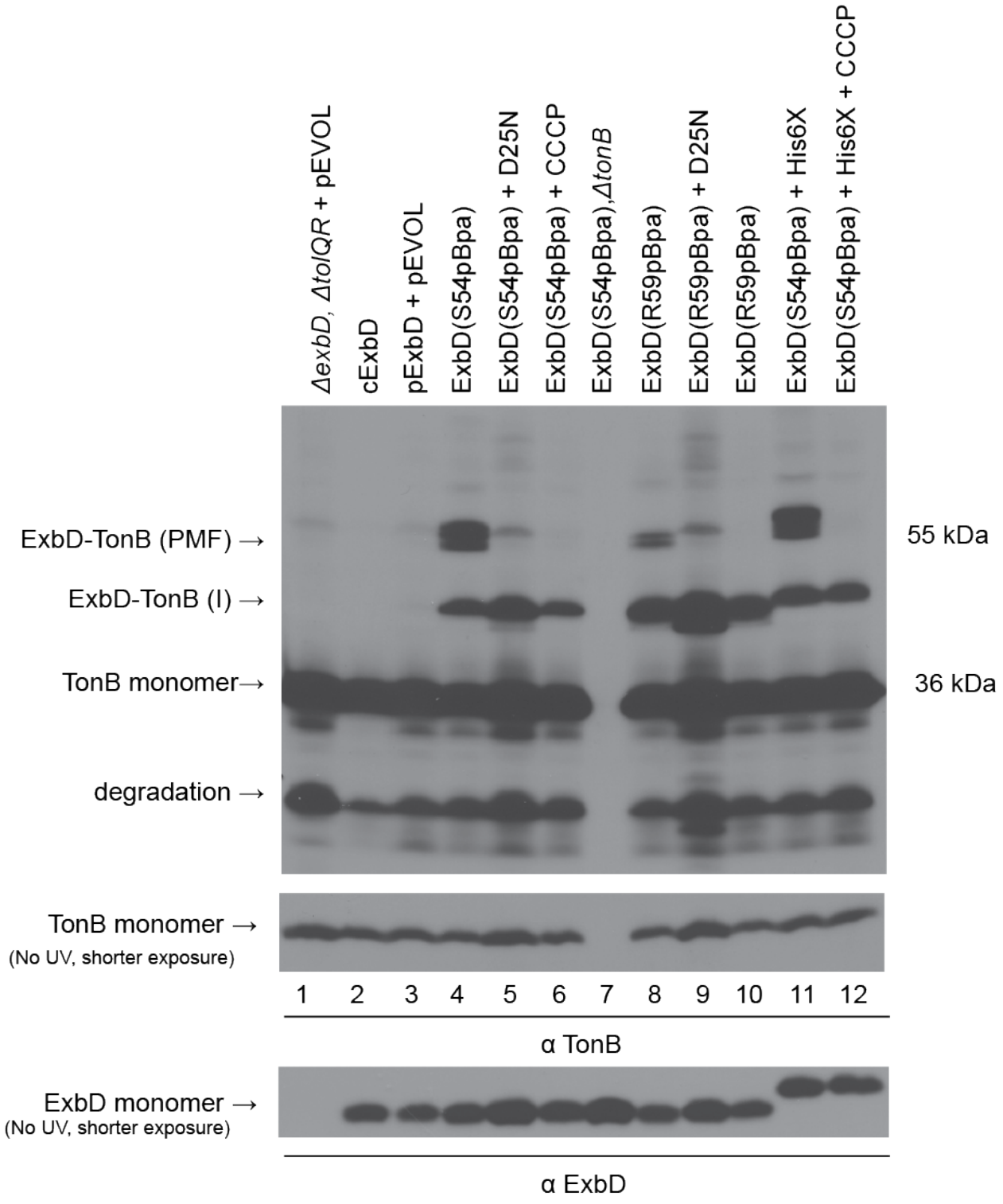

Figure 3: Identification of ExbD-TonB PMF-dependent and PMF-independent complexes using *in vivo* photo-cross-linking. Plasmid-encoded ExbD (pBpa) substitutions were co-expressed with pEVOL in strain RA1045 (Δ*exbD*, Δ*tolQR*). At mid-exponential phase, strains were subjected to UV irradiation for photo-cross-linking as described in Materials and Methods.

1072 Equivalent numbers of cells were precipitated with TCA and the ExbD-TonB complexes were
1073 visualized on immunoblots of 13% SDS-polyacrylamide gels with anti-TonB monoclonal
1074 antibodies. cExbD designates chromosomally expressed ExbD from the wild-type strain,
1075 W3110. The parent plasmid strain pExbD (pKP999) and all ExbD (pBpa) substitutions were
1076 expressed in RA1045 (Δ*exbD*, Δ*tolQR*), except for ExbD (S54pBpa) ΔtonB, which was
1077 expressed in KP1509 (Δ*exbD*, Δ*tolQR, ΔtonB*). D25N is a mutation in the ExbD TMD. The
1078 protonophore CCCP was added prior to UV exposure. His6X refers to ExbD (S54pBpa) with a
1079 C-terminal His6X tag. On the left, positions of a PMF-dependent ExbD-TonB complex [ExbD-
1080 TonB (PMF], a PMF-independent complex [ExbD-TonB (I)], monomeric TonB, and a TonB
1081 degradation product are shown. Mass markers are indicated on the right. Steady state ExbD
1082 and TonB monomer levels from the same experiment were determined by immunoblot analysis
1083 of control samples that were not exposed to UV light. The plasmid identities and
1084 concentrations of propionate for chromosomal expression are listed in Table S1.

1085
1086
1087
1088
1089
1090
1091
1092
1093
1094
1095
1096
1097

1098 **A.**

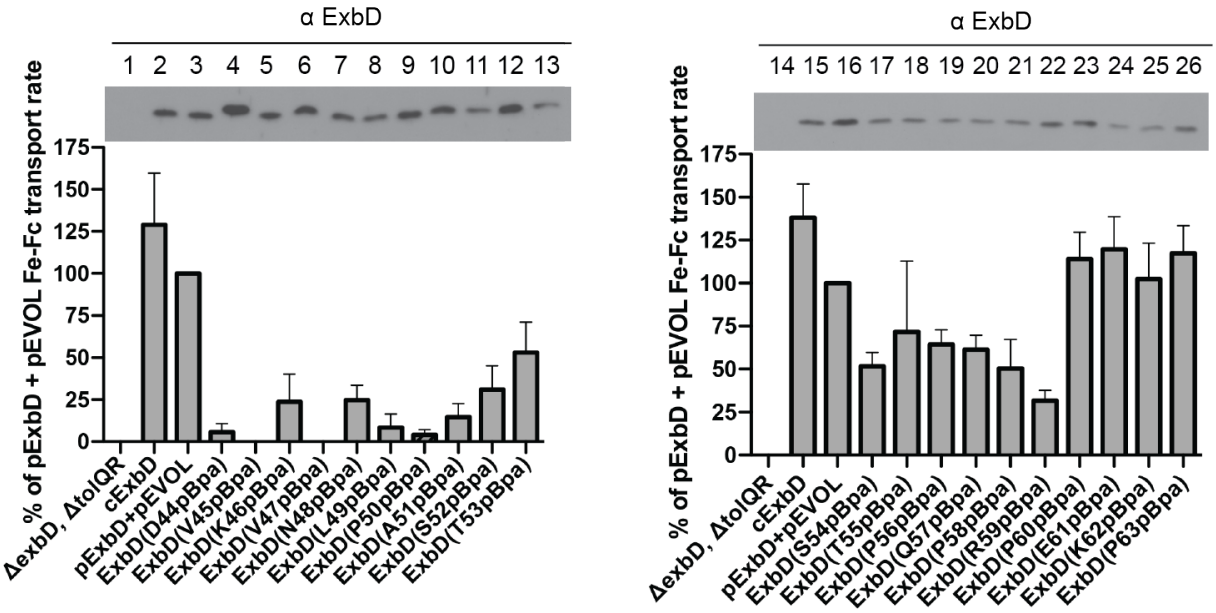

1099

1100 **B.**

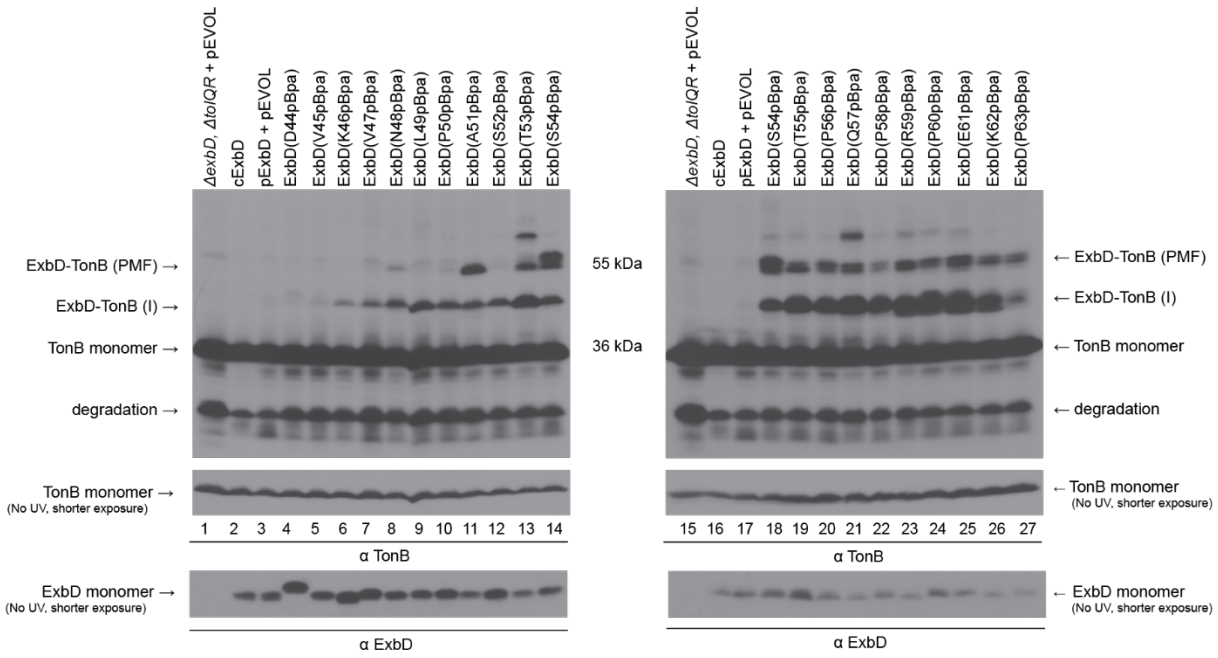

1101

1102

1103 **Figure 4: Virtually all the ExbD (pBpa) substitutions in the ExbD disordered region**

1104 **capture PMF-dependent or PMF-independent TonB complexes.** (A) Initial rate of ^{55}Fe-

1105 ferrichrome transport for ExbD (pBpa) substitutions at residues 44-54 (left panel) and residues

1106 54-63 (right panel) with the corresponding steady-state expression levels of ExbD proteins at

1107 the time of assay above each panel. ExbD pBpa substitutions were plasmid-encoded and co-
1108 expressed with plasmid pEVOL in RA1045 (Δ*exbD*, Δ*tolQR*). Strains were grown to mid-
1109 exponential phase and assayed as described in Methods and Materials. The percentages of
1110 activity were calculated relative to the initial rate for ^{55}Fe-ferrichrome transport of plasmid-
1111 encoded ExbD, pExbD (pKP999). Assays were performed in triplicate and carried out at least
1112 twice for each strain. The slopes were determined by a linear regression fit of scintillation
1113 counts per minute. The error bars indicate mean ± SEM for a representative triplicate set.
1114 cExbD designates chromosomally expressed ExbD from the wild-type strain, W3110. The
1115 plasmid identities and concentrations of propionate for chromosomal expression are listed in
1116 Table S1. (B) *In vivo* photo-cross-linking of pBpa substitutions for ExbD residues 44-54 (left
1117 panel) and residues 54-63 (right panel) on an anti-TonB immunoblot. Note that ExbD
1118 S54)pBpa is included on both immunoblots in lanes 14 and 18 for comparison of levels of
1119 expression. All samples (identical as in A) were grown to mid-exponential phase, at which
1120 point photo-cross-linking was performed as described in Materials and Methods. Equivalent
1121 numbers of cells were precipitated with TCA and the ExbD-TonB complexes were visualized
1122 on immunoblots of 13% SDS-polyacrylamide gels with anti-TonB monoclonal antibodies. On
1123 the left and right, positions of a PMF-dependent ExbD-TonB complex [ExbD-TonB (PMF)], a
1124 PMF-independent complex [ExbD-TonB (I)], monomeric TonB, and a TonB degradation
1125 product are shown. Mass markers are indicated in the center. The steady-state ExbD and
1126 TonB monomer levels from the same experiment were determined by immunoblot analysis of
1127 control samples that were not exposed to UV light.

1128

1129

1130

1131

1132

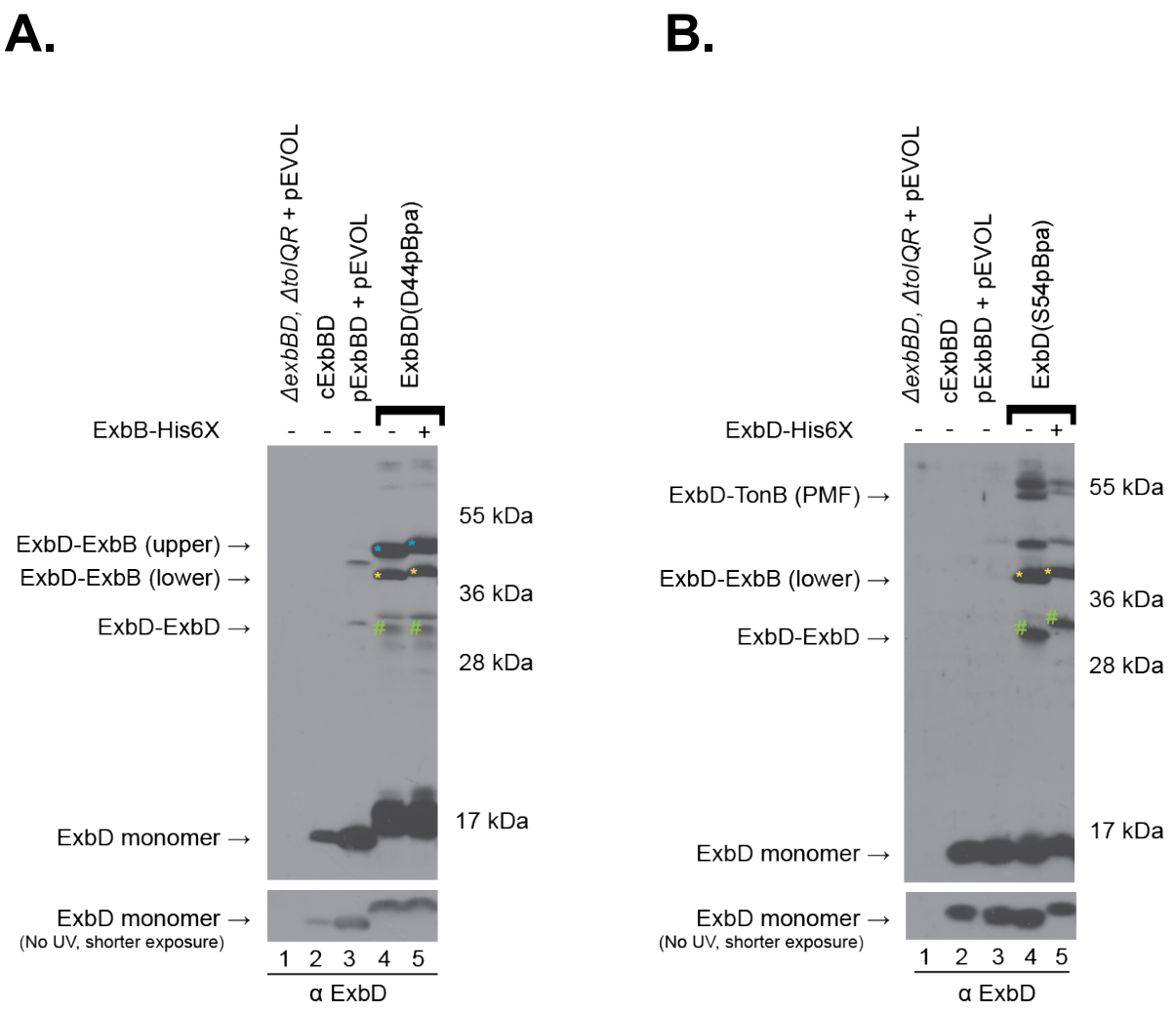

1133

1134 **Figure 5: Two different ExbD-ExbB complexes and an ExbD homodimer are identified by**
1135 ***in vivo* photo-cross-linking**. (A) *In vivo* photo-cross-linking of a representative ExbD photo-
1136 cross-linkable mutant, ExbD (D44pBpa), in the presence of ExbB with (+) and without (-) a C-
1137 terminal His6X-tag. At mid-exponential phase, strains were subjected to UV irradiation for
1138 photo-cross-linking as described in Materials and Methods. Equivalent numbers of cells were
1139 precipitated with TCA and the ExbD complexes were visualized on immunoblots of 13% SDS-
1140 polyacrylamide gels with anti-ExbD polyclonal antibodies. cExbD designates chromosomally
1141 expressed ExbB and ExbD from the wild-type strain, W3110. Plasmid pExbBD (pKP1657) and
1142 its corresponding ExbD (D44pBpa) variants were expressed with pEVOL in RA1017 (W3110,
1143 *ΔexbBD::kan, ΔtolQRA*). ExbD is overexpressed from plasmid pExbBD and its corresponding

1144 ExbD (D44pBpa) variant in the absence of inducer relative to chromosomally ExbD
1145 expression. Positions of ExbD-ExbB (upper)—blue asterisk on immunoblot, ExbD-ExbB
1146 (lower)—yellow asterisk on immunoblot, likely ExbD-ExbD homodimers–green pound symbol
1147 on immunoblot, and ExbD monomer are indicated on the left. pExbBD expressed with pEVOL
1148 (lane 3) forms two unidentified complexes that are non-ExbD residue-specific (unlabeled).
1149 Mass markers are indicated on the right. Steady-state ExbD monomer levels from the same
1150 experiment were determined by immunoblot analysis of control samples that were not exposed
1151 to UV light. The plasmid identities and concentrations of propionate for chromosomal
1152 expression are listed in Table S1. (B) *In vivo* photo-cross-linking of ExbD (S54pBpa), with (+)
1153 and without (-) a C-terminal His6X-tag using the same procedure as in (A). Plasmid pExbD
1154 (pKP999) and a corresponding variant, ExbD (S54pBpa) were expressed with pEVOL in
1155 RA1045 (Δ*exbD*, Δ*tolQR*). On the left, positions of a PMF-dependent ExbD-TonB complex
1156 [ExbD-TonB (PMF], ExbD-ExbB, an ExbD homodimer, and monomeric ExbD are shown. Mass
1157 markers are indicated on the right. Steady-state ExbD monomer levels from the same
1158 experiment were determined by immunoblot analysis of control samples that were not exposed
1159 to UV light. The plasmid identities and concentrations of propionate for chromosomal
1160 expression are listed in Table S1.

1161

1162

1163

1164

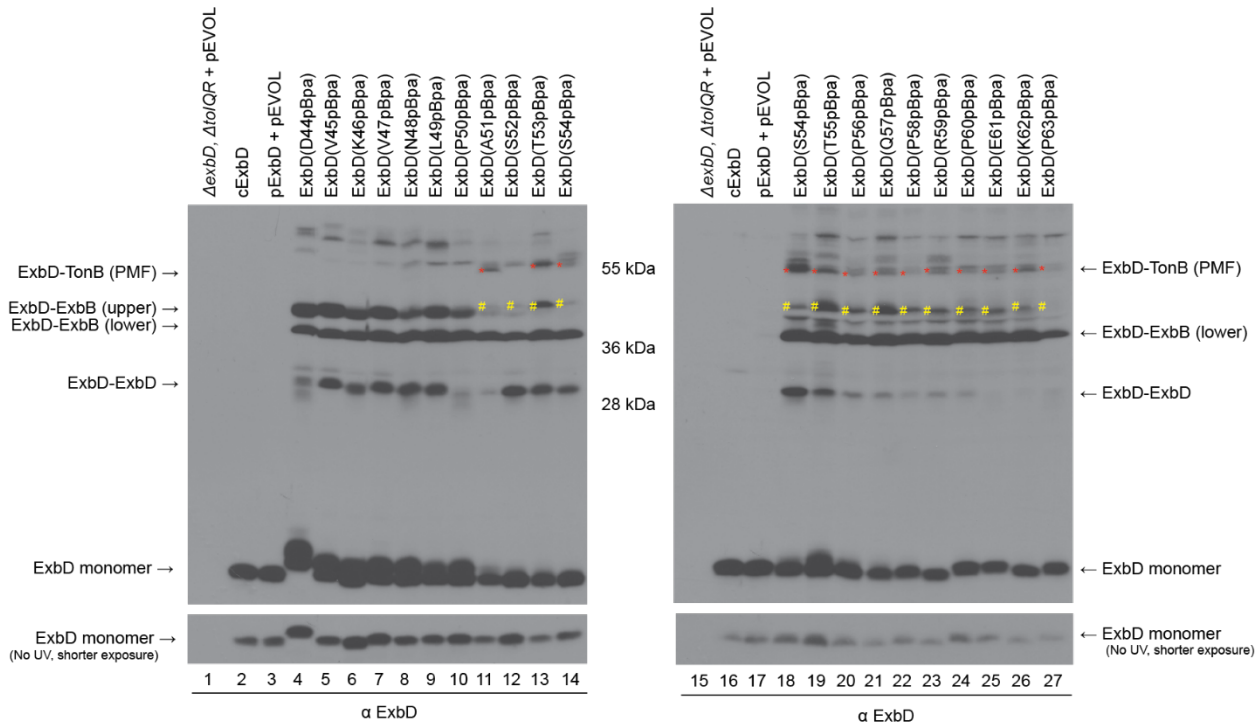

Figure 6: The majority of pBpa substitutions in the ExbD disordered region capture contacts with ExbB and ExbD. *In vivo* photo-cross-linking of ExbD pBpa substitutions in residues 44-54 (left panel) and 54-63 (right panel) from Fig. 4 probed with anti-ExbD antibodies. Note that ExbD (S54pBpa) is included on both immunoblots in lanes 14 and 18 for comparison of levels of expression. Strains were grown to mid-exponential phase, at which point photo-cross-linking was performed as described in Materials and Methods. Equivalent numbers of cells were precipitated with TCA and the ExbD-TonB complexes were visualized on immunoblots of 13% SDS-polyacrylamide gels with anti-ExbD polyclonal antibodies. cExbD designates chromosomally expressed ExbD from the wild-type strain, W3110. Plasmid pExbD (pKP999) and its corresponding ExbD pBpa substitutions were expressed in RA1045 (Δ*exbD*, Δ*tolQR*) with plasmid pEVOL. Positions of the PMF-dependent ExbD-TonB complex identified in Fig. 3, ExbD-ExbB (upper) and ExbD-ExbB (lower) from Figure 5A, the ExbD-ExbD from Figure 5B and ExbD monomer are indicated on the right and left. The ExbD-TonB (PMF) is differentiated from unknown complexes by a red asterisk (*). The ExbD-TonB PMF-

1181 independent complex is distinguished from ExbB-ExbD (upper) by a yellow pound symbol (#).
1182 Mass standards are in the center. The steady-state ExbD levels from the same experiment
1183 were determined by immunoblot analysis of control samples that were not exposed to UV light
1184 (bottom). The plasmid identities and concentrations of propionate for chromosomal expression
1185 are listed in Table S1.

1186

1187

1188

1189

1190

1191

1192

1193

1194

1195

1196

1197

1198

1199

A.

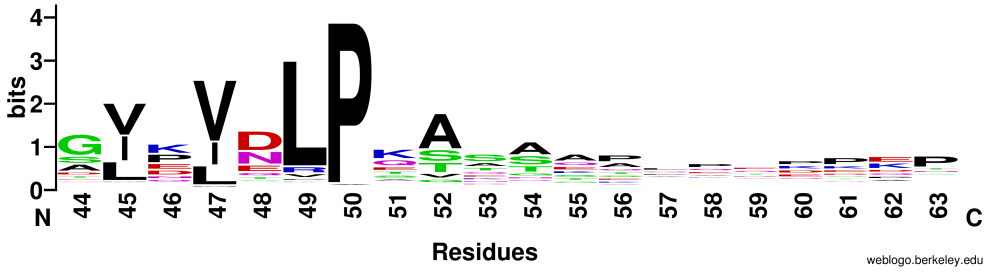

B.

```
CLUSTAL multiple sequence alignment by MUSCLE (3.8)

ExbD (38) ---APLATVDVKVNLPASTSTPQPRPE------------KPVYLSVKA--------(60)
TolR (36) ---APIITQSVEVDLPDATESQAVSSNDN----------PPVIVEVSG--------(60)
MotB (61) YFRTPLATAVTGGDRISNSESPIPGGGDDYTQSQGEVNKQPNIEELKKRMEQSRLR (116)
  :*: * . : :.:  * .:.
```

Figure 7: A conservation alignment of the ExbD disordered region identifies a ΨXΨXLP motif. The psi symbol (Ψ) represents a residue with a large aliphatic side chain and X represents any non-hydrophobic residue. (A) A WebLogo image of the ExbD disordered region. The image was generated from an ExbD multiple sequence alignment by HHblits of sequences within an E-value of e^{-10} of *Escherichia coli K-12* strain (NP_417478.1) using the Gremelin.bakerlab program (gremlin.bakerlab.org/). Positions with >75% sequences alignment gaps were removed. (B) A multiple sequence alignment was used to identify potential ΨXΨXLP motifs in ExbD homologs TolR and MotB. A clustal multiple sequence alignment was generated by MUSCLE (3.8) of *Escherichia coli* ExbD (AAA69172.1), TolR (PSM33938.1), and MotB (ACB03086.1). A red box encompasses the *Escherichia coli* K12 ExbD ΨXΨXLP motif containing conserved residues V45, V47, L49 and P50 and shows that these residues are conserved in TolR but not MotB.

A.

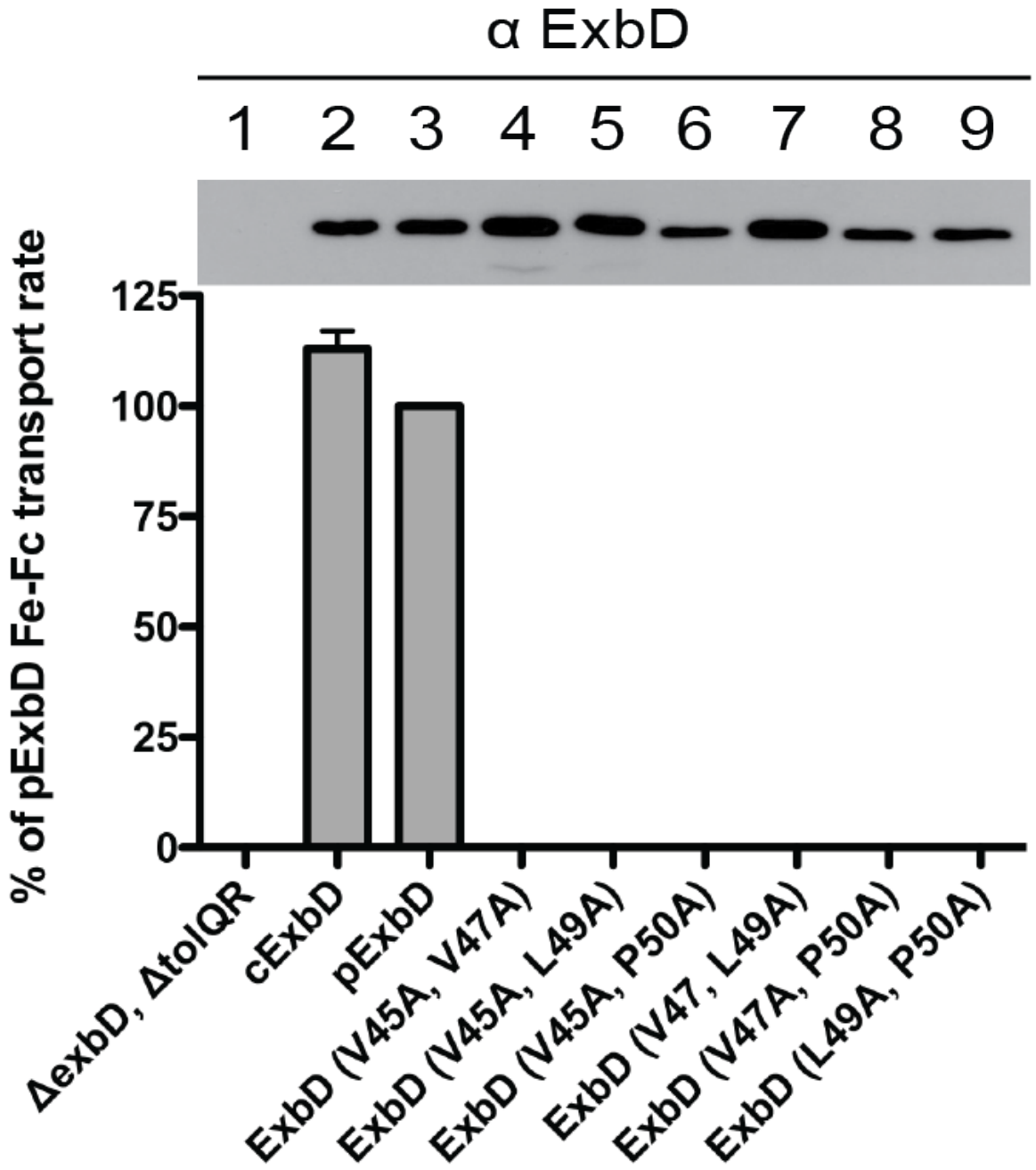
α ExbD
1 2 3 4 5 6 7 8 9
% of pExbD Fe-Fc transport rate
125
100
75
50
25
0
ΔexbD, ΔtolQR
cExbD
pExbD
ExbD (V45A, V47A)
ExbD (V45A, L49A)
ExbD (V45A, P50A)
ExbD (V47 , L49A)
ExbD (V47A, P50A)
ExbD (L49A, P50A)

1224

B.

Mutant	Colicin B+	Colicin Ia+	Colicin M+
pExbD	8, 9, 8	8, 8, 8	8, 8, 8
ExbD (V45A, V47A)	T, T, T	T, T, T	T, T, T
ExbD (V45A, L49A)	T, T, T	T, T, T	T, T, T
ExbD (V45A, P50A)	T, T, T	0*, 0*, 0*	T, T, T
ExbD (V47A, L49A)	T, T, T	T, T, T	T, T, T
ExbD (V47A, P50A)	T, T, T	T, T, T	T, T, T
ExbD (L49A, P50A)	T, T, T	T, T, T	T, T, T

+ T refers to tolerant to undiluted colicin lysate
* 0 refers to hazy clearing in with undiluted colicin

1225

1226 **Figure 8: The synergy of double-alanine substitutions within the ExbD ΨXΨXLP motif**

1227 **establishes its essentiality for TonB-dependent energy transduction.**

1228 Initial rate of ^{55}Fe-ferrichrome transport for ExbD variants with the corresponding steady-state

1229 expression levels of ExbD proteins at the time of assay above each panel. Strains were grown

1230 to mid-exponential phase and assayed as described in Methods and Materials. The

1231 percentages of activity were calculated relative to the initial rate for ^{55}Fe-ferrichrome transport

1232 of plasmid-encoded ExbD, pExbD (pKP999). Assays were performed in triplicate and carried

1233 out at least twice for each strain. The slopes were determined by a linear regression fit of

1234 scintillation counts per minute. The error bars indicate mean ± SEM for a representative

1235 triplicate set (above). Steady-state levels of ExbD-specific expression from the transport

1236 experiments are indicated above the corresponding bars of the graph below them. cExbD

1237 designates chromosomally expressed ExbD from the wild-type strain, W3110. The plasmid

1238 identities and concentrations of propionate for chromosomal expression are listed in Table S1.
1239 (B) Colicin sensitivity assay. Strains were grown to mid-exponential phase and assayed in
1240 triplicate with Colicin B, Colicin Ia, and Colicin M as described in the Material and Methods.
1241 pExbD (pKP999) and all ExbD alanine substitutions were expressed from plasmids in RA1045
1242 (Δ*exbD*, Δ*tolQR*). The plasmid identities and concentrations of propionate for chromosomal
1243 expression are listed in Table S1. Scoring was reported as the highest 5-fold colicin dilution
1244 that produced clearing in three different trials. “T” refers to colicin tolerance (insensitivity) and
1245 “0” refers to hazy clearing caused by the undiluted colicin lysate.

1246

1247

1248

1249

1250

1251

1252

1253

1254

1255

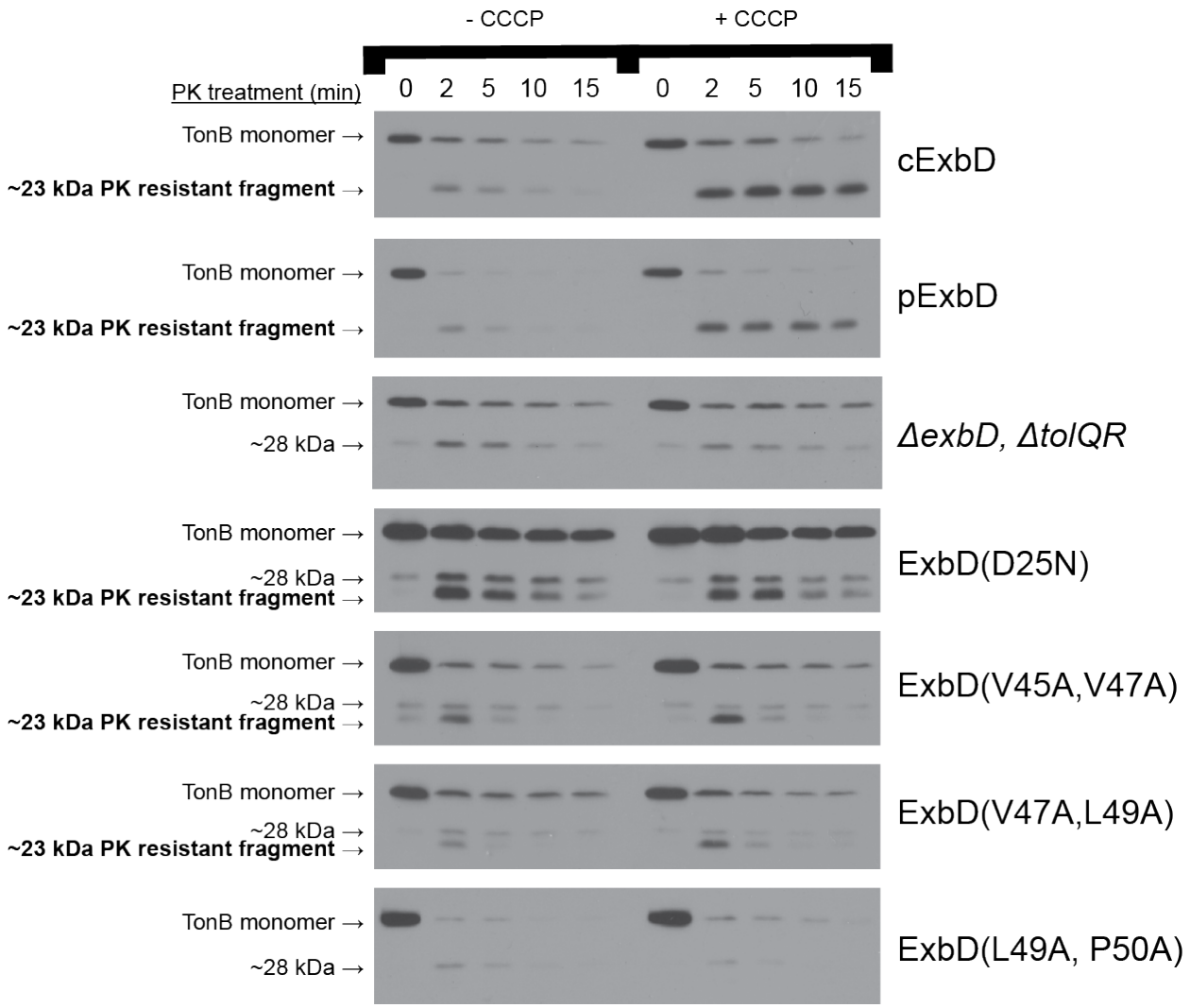

Figure 9: Mutations in the ExbD ΨXΨXLP motif leave TonB stalled at Stage II when PMF is present. Spheroplasts were generated from W3110 (cExbD), and RA1045 (Δ*exbD*, Δ*tolQR*), as well as RA1045 containing plasmids pKP999 (pExbD), pKP1194 [ExbD (D25N)], pKP2171 [ExbD (V45A, V47A)], pKP2201 [ExbD (V47A, L49A)], and pKP2202 [ExbD (L49A, P50A)] as described in the Materials and Methods. Each spheroplast was treated with proteinase K (PK) for 0 min, 2 min, 5 min, 10 min and 15 min in the presence of DMSO (-CCCP) or CCCP dissolved in DMSO (+CCCP). The samples were visualized on immunoblots of 13% SDS-polyacrylamide gels with anti-TonB monoclonal antibodies. Identities of the various strains assayed are indicated on the left. Positions of TonB monomers, the ~23 kDa

1267 PK-resistant TonB fragment indicative of Stage II of TonB energization and the ~28 kDa
1268 fragment with no known relevance to any Stage in the TonB energization cycle (34), are on the
1269 left. The appearance of the ~23 kDa TonB fragment upon lengthy exposure of ExbD (L49A,
1270 P50A) samples allowed confident identification of the 28 kDa TonB fragment generated in that
1271 strain. The concentrations of propionate for chromosomal expression are listed in Table S1.

1272

1273

1274

1275

1276

1277

1278

1279

1280

1281

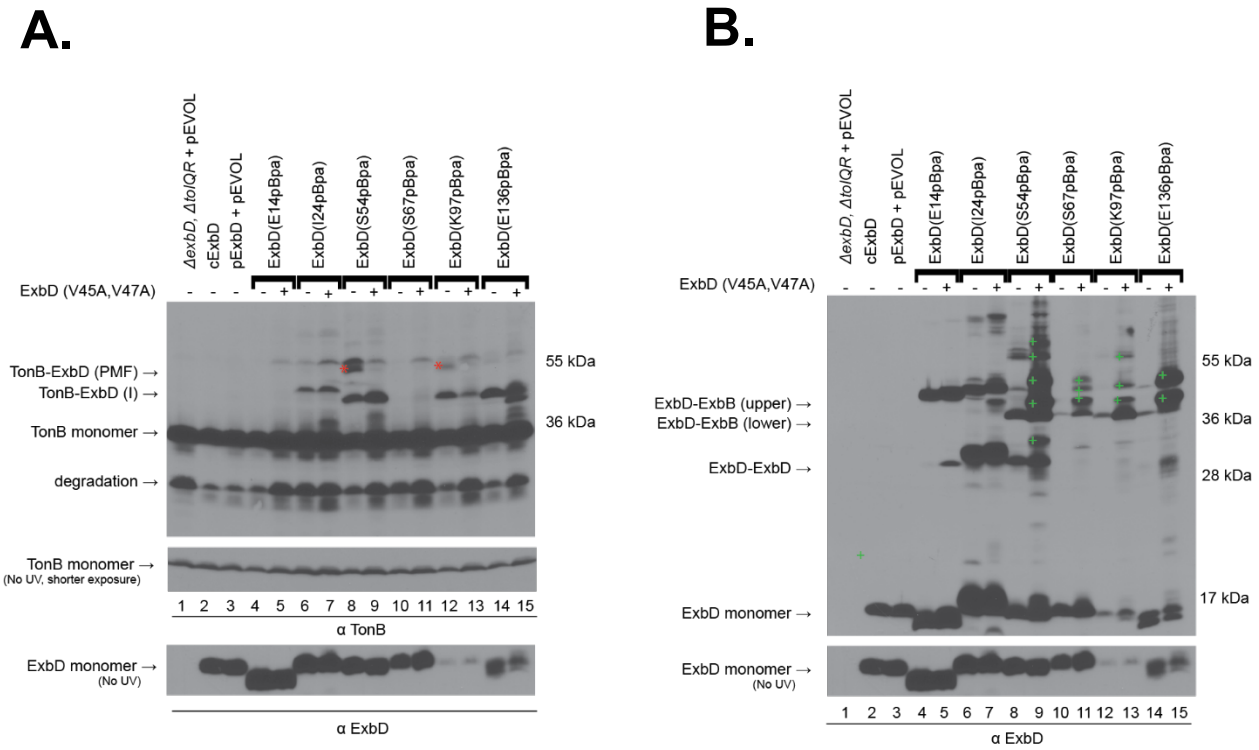

Figure 10: The ExbD ΨXΨXLP motif controls ExbD interactions through other sites. *In vivo* photo-cross-linking of ExbD (E14pBpa), ExbD (I24pBpa), ExbD (S54pBpa), ExbD (S67pBpa), ExbD (K97pBpa), and ExbD (E136pBpa) with (+) and without (-) V45A,V47A double alanine substitutions. Strains were grown to mid-exponential phase, at which point photo-cross-linking was performed as described in Materials and Methods. Equivalent numbers of cells were precipitated with TCA and the samples were visualized on immunoblots of 13% SDS-polyacrylamide gels with either (A) anti-TonB monoclonal antibodies or (B) anti-ExbD polyclonal antibodies. cExbD designates chromosomally expressed ExbD from the wild-type strain, W3110. The parent plasmid pExbD (pKP999) and corresponding ExbD variants were co-expressed with plasmid pEVOL in RA1045 (Δ*exbD*, Δ*tolQR*). (A) On the left, positions of a PMF-dependent ExbD-TonB complex [ExbD-TonB (PMF)—red asterisk], a PMF-independent complex [ExbD-TonB (I)], monomeric TonB, and a TonB degradation product are shown (See Fig. 3). Mass markers are indicated on the right. Steady state ExbD and TonB

1297 monomer levels from the same experiment were determined by immunoblot analysis of control
1298 samples that were not exposed to UV light. (B) On the left, positions of ExbD-ExbB (upper)
1299 and ExbD-ExbB (lower) (see Figure 5A), the ExbD-ExbD homodimer (see Figure 5B) and
1300 ExbD monomer are shown. Unidentified complexes trapped by the ExbD pBpa variants
1301 containing V45A,V47A are indicated on the immunoblot by a green (+) symbol. Mass markers
1302 are indicated on the right. Steady-state ExbD levels from the same experiment were
1303 determined by immunoblot analysis of control samples that were not exposed to UV light. The
1304 plasmid identities and concentrations of propionate for chromosomal expression are listed in
1305 Table S1.

1306

1307

1308

1309

1310

1311

1312

1313

1314

1315

1316

1317

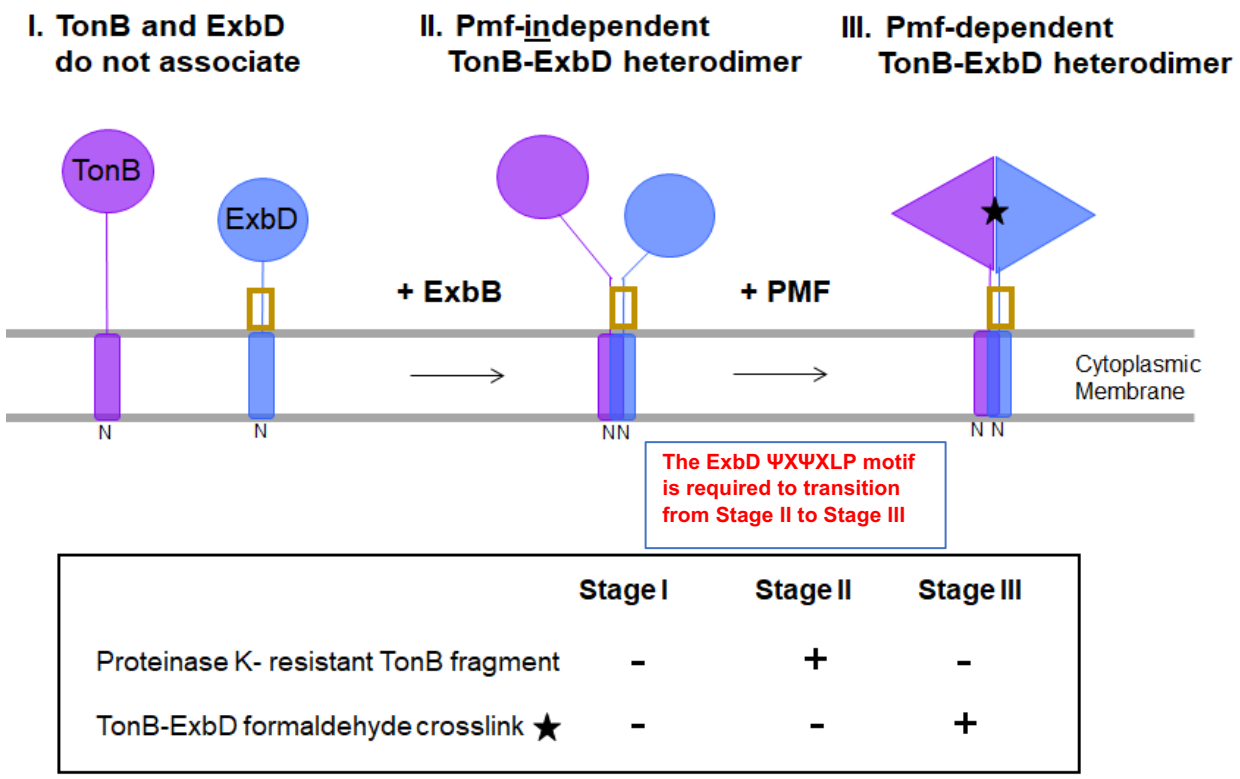

Figure 11: Model: The PMF-dependent transition from Stage II to Stage III requires the ExbD ΨXΨXLP motif. Initial Stages of TonB energization. The *in vivo* data suggest that the C-terminus of TonB is an intrinsically disordered protein whose conformation is managed by ExbD [(34), Fig. 1]. In Stage I, ExbD and TonB do not interact, although both are stabilized by ExbB (not shown). TonB in untreated spheroplasts is degraded by exogenously added proteinase K. In Stage II, the first ~155 residues of TonB are somehow protected from proteinase K if the spheroplasts have been treated with the protonophore CCCP and if ExbD is also present. The protonophore CCCP is required to prevent TonB transitioning to Stage III. Although we hypothesized at that time that ExbD was protecting TonB, no Stage II complex containing both proteins was detected.

In this study, we captured for the first time the ExbD-TonB PMF-independent intermediate using *in vivo* photo-cross-linking as part of the normal energy transduction cycle, without the need to add protonophore. Mutations in the ExbD ΨXΨXLP motif (gold box)

1333 allowed capture of ExbD-TonB in Stage II, but prevented transition of TonB to Stage III. In
1334 Stage III, ExbD and TonB can be formaldehyde cross-linked into a PMF-dependent complex
1335 containing both proteins and in this work we also capture the Stage III, PMF-dependent form of
1336 ExbD-TonB. This figure was adapted from Gresock et al, 2015 (26).

1337

1338

1339

1340

1341

1342

1343

1344

1345

1346

1347

1348

1349

1350

1351

1352

1353 # SUPPLEMENTAL INFORMATION

1354 ## Table S1, Kopp and Postle:

Strain	**Genotype**		**Reference**
W3110	F^- IN(*rrnD-rrnE*)*1*		(1)
KP1270	W3110, *aroB-*		(2)
RA1045	W3110, Δ*exbD*, Δ*tolQR*		(3)
KP1526	W3110, Δ*exbD*, Δ*tolQR, aroB-*		Present Study
RA1017	W3110, Δ*exbBD*::*kan*, Δ*tolQRA*		(4)
KP1509	W3110 Δ*exbD* Δ*tolQR,* Δ*tonB*::*kan*		(5)
Plasmid	**Genotype or Phenotype**	**[a]Propionate Induction Concentration**	**References**
pEVOL-BpF	tRNA synthetase and tRNA for pBpa, camr , p15A	N/A	(6)
pKP999	*exbD* in pPro24	0.5 mM	(5)
pKP1657	*exbBD* in pPro24	0 mM	Present study
pKP1064	*ExbD (D25N)*	0 mM	(5)
pKP2073	ExbD (44-48ala)	0.25 mM	Present study
pKP2077	ExbD (49-53ala)	0.5 mM	Present study
pKP2153	ExbD (54-58ala)	0.75 mM	Present study
pKP2180	ExbD (59-63ala)	20 mM	Present study
pKP2140	ExbD (D44A)	0.25 mM	Present study
pKP2141	ExbD (V45A)	2.5 mM	Present study
pKP2142	ExbD (K46A)	0 mM	Present study
pKP2143	ExbD (V47A)	1 mM	Present study

pKP2144	ExbD (N48A)	0.25 mM	Present study
pKP2145	ExbD (L49A)	0.25 mM	Present study
pKP2154	ExbD (P50A)	0 mM	Present study
pKP2152	ExbD (S52A)	0.25 mM	Present study
pKP2146	ExbD (T53A)	0.25 mM	Present study
pKP2007	ExbD (D44Am)	0 mM	Present study
pKP2133	ExbD (V45Am)	0 mM	Present study
pKP2017	ExbD (K46Am)	0 mM	Present study
pKP2131	ExbD (V47Am)	0.5 mM	Present study
pKP2018	ExbD (N48Am)	2 mM	Present study
pKP2147	ExbD (L49Am)	0.5 mM	Present study
pKP1971	ExbD (P50Am)	0 mM	Present study
pKP2138	ExbD (A51Am)	45 mM	Present study
pKP1951	ExbD (S52Am)	1 mM	Present study
pKP2151	ExbD (T53Am)	1 mM	Present study
pKP1972	ExbD (S54Am)	1 mM	Present study
pKP2139	ExbD (T55Am)	8 mM	Present study
pKP1973	ExbD (P56Am)	5 mM	Present study
pKP2137	ExbD (Q57Am)	10 mM	Present study
pKP1974	ExbD (P58Am)	5 mM	Present study
pKP1898	ExbD (R59Am)	5 mM	Present study
pKP1975	ExbD (P60Am)	8 mM	Present study
pKP2027	ExbD (E61Am)	10 mM	Present study
pKP1949	ExbD (K62Am)	8 mM	Present study

pKP2136	ExbD (P63Am)	7 mM	Present study
pKP1926	ExbD (E14Am)	4 mM	Present study
pKP2064	ExbD (I24Am)	0 mM	Present study
pKP2167	ExbD (S67Am)	5 mM	Present study
pKP2227	ExbD (K97Am)	2 mM	Present study
pKP1907	ExbD (E136Am)	0 mM	Present study
pKP2171	ExbD (V45A, V47A)	1 mM	Present study
pKP2164	ExbD (V45A, L49A)	0.5 mM	Present study
pKP2182	ExbD (V45A, P50A)	0.25 mM	Present study
pKP2201	ExbD (V47A, L49A)	0.25 mM	Present study
pKP2190	ExbD (V47A, P50A)	0.25 mM	Present study
pKP2202	ExbD (L49A, P50A)	0.5 mM	Present study
pKP2213	ExbD (V45A,V47A, E14Am)	0 mM	Present study
pKP2214	ExbD (V45A,V47A, I24Am)	0 mM	Present study
pKP2161	ExbD (V45A,V47A, S54Am)	3 mM	Present study
pKP2215	ExbD (V45A,V47A, S67Am)	1.5 mM	Present study
pKP2228	ExbD (V45A,V47A, K97Am)	30 mM	Present study
pKP2220	ExbD (V45A,V47A, E136Am)	0 mM	Present study
pKP2063	ExbD (S54pBpa, D25N)	1 mM	Present study
pKP1932	ExbD (R59pBpa, D25N)	5 mM	Present study
pKP2259	ExbD (S54AM)-His(6x)	5mM	Present study
pKP2295	ExbB-ExbD (D44Am)	0 mM	Present study
pKP2272	ExbB-His(6x)-ExbD (D44Am)	0 mM	Present study

1355 [a] Propionate concentration required for plasmid induction in RA1045 background strain to
1356 achieve similar W3110 ExbD chromosomal protein levels.

SUPPLEMENTAL FIGURES Kopp and Postle:

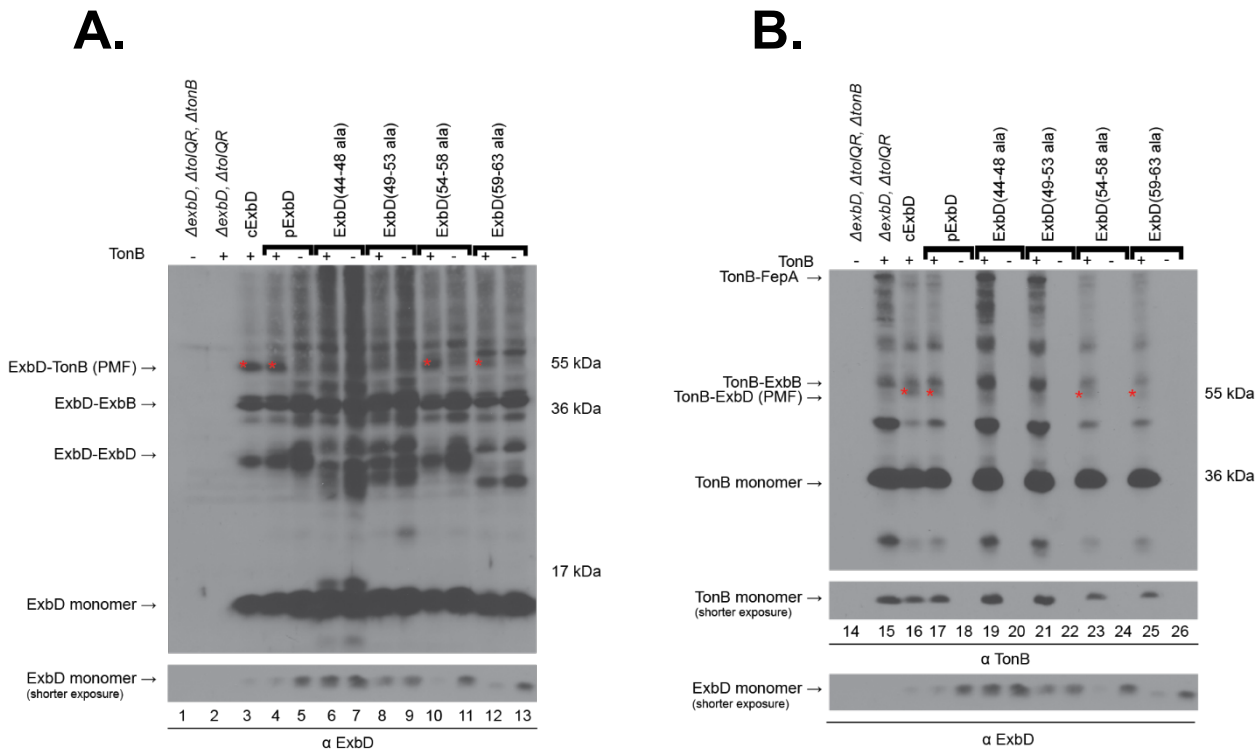

Figure S1: ExbD (44-48ala) and ExbD (49-53ala) fail to form a formaldehyde crosslinked ExbD-TonB PMF-dependent complex. *In vivo* formaldehyde-cross-linking of block alanine substitutions in the ExbD disordered region. Strains were grown to mid-exponential phase, at which point formaldehyde-cross-linking was performed as described in Materials and Methods. Equivalent numbers of cells were visualized on immunoblots of 13% SDS-polyacrylamide gels with (A) anti-ExbD polyclonal and (B) anti-TonB monoclonal antibodies. cExbD designates chromosomally expressed ExbD from the wild-type strain, W3110. The parent plasmid, pExbD (pKP999) and its corresponding ExbD block alanine substitutions were expressed in both RA1045 (Δ*exbD*, Δ*tolQR*) [+] and KP1509 (Δ*exbD*, Δ*tolQR,* Δ*tonB*) [-]. (A) Positions of the

1371 previously characterized formaldehyde cross-linked PMF-dependent ExbD-TonB complex (red
1372 asterisk on immunoblot), the ExbD-ExbB complex, the ExbD-ExbD homodimer and ExbD
1373 monomer are shown on the left (5). Mass markers are shown on the right. (B) Positions of the
1374 TonB-FepA complex, the TonB-ExbB complex, the PMF-dependent TonB-ExbD complex and
1375 TonB monomer are shown. Mass markers are shown on the right. Below each immunoblot are
1376 the levels of the corresponding monomer in each sample. The plasmid identities and
1377 concentrations of propionate for chromosomal expression are listed in Table S1.

1378

1379

1380

1381

1382

1383

1384

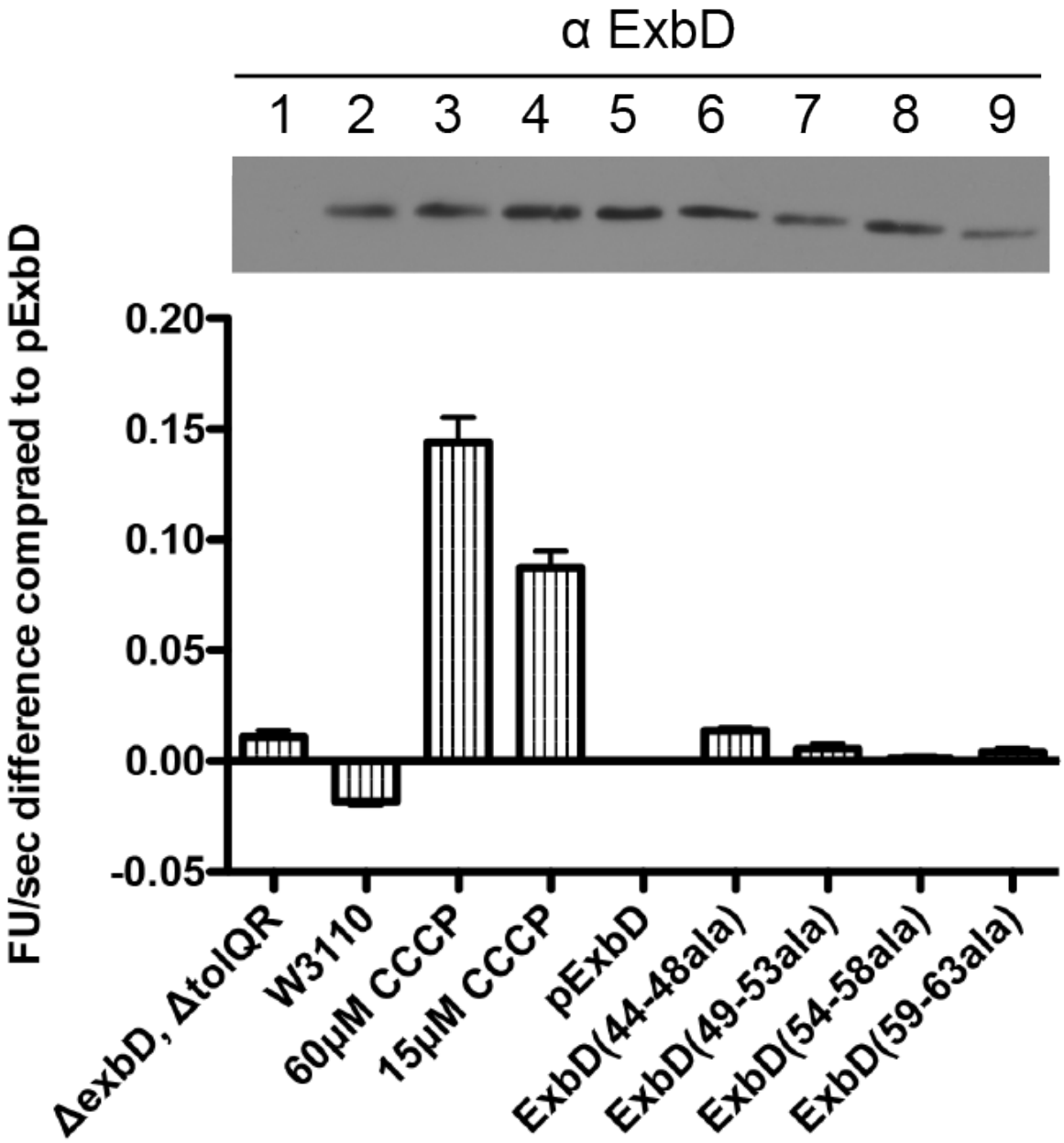

1385

1386 **Figure S2: Failure to form the PMF-dependent ExbD-TonB formaldehyde crosslink is not**
1387 **due to loss of PMF; a small, but significant difference is detected among the block ala**
1388 **substitutions.** The rate of ethidium bromide (EtBr) accumulation, an indirect assay for loss of
1389 PMF, was measured for ExbD alanine block substitutions as described in the Materials and
1390 Methods. Strains were grown to mid-exponential phase and assayed as described in Methods
1391 and Materials. (A) The average EtBr accumulation rates (FU/sec) were calculated relative to
1392 the rate of plasmid-encoded ExbD, pExbD (pKP999) expressed at chromosomal levels in

1393 RA1045 (Δ*exbD*, Δ*tolQR*). The corresponding steady-state ExbD monomer levels determined
1394 by immunoblot analysis from the experiment from one of the trials are shown above the bar
1395 graph. cExbD designates chromosomally expressed ExbD from the wild-type strain, W3110.
1396 For lanes 3 and 4, W3110 was treated with 60 μM CCCP or 15 μM (as labeled) was prior to
1397 addition of EtBr as described in the Materials and Methods. ExbD alanine substitutions were
1398 expressed from plasmids in RA1045 (Δ*exbD*, Δ*tolQR*). The plasmids and concentrations of
1399 propionate for chromosomal expression are listed in Table S1. Numbers above the immunoblot
1400 correspond to samples below them starting with (Δ*exbD*, Δ*tolQR*) on the left as #1.

1401

1402

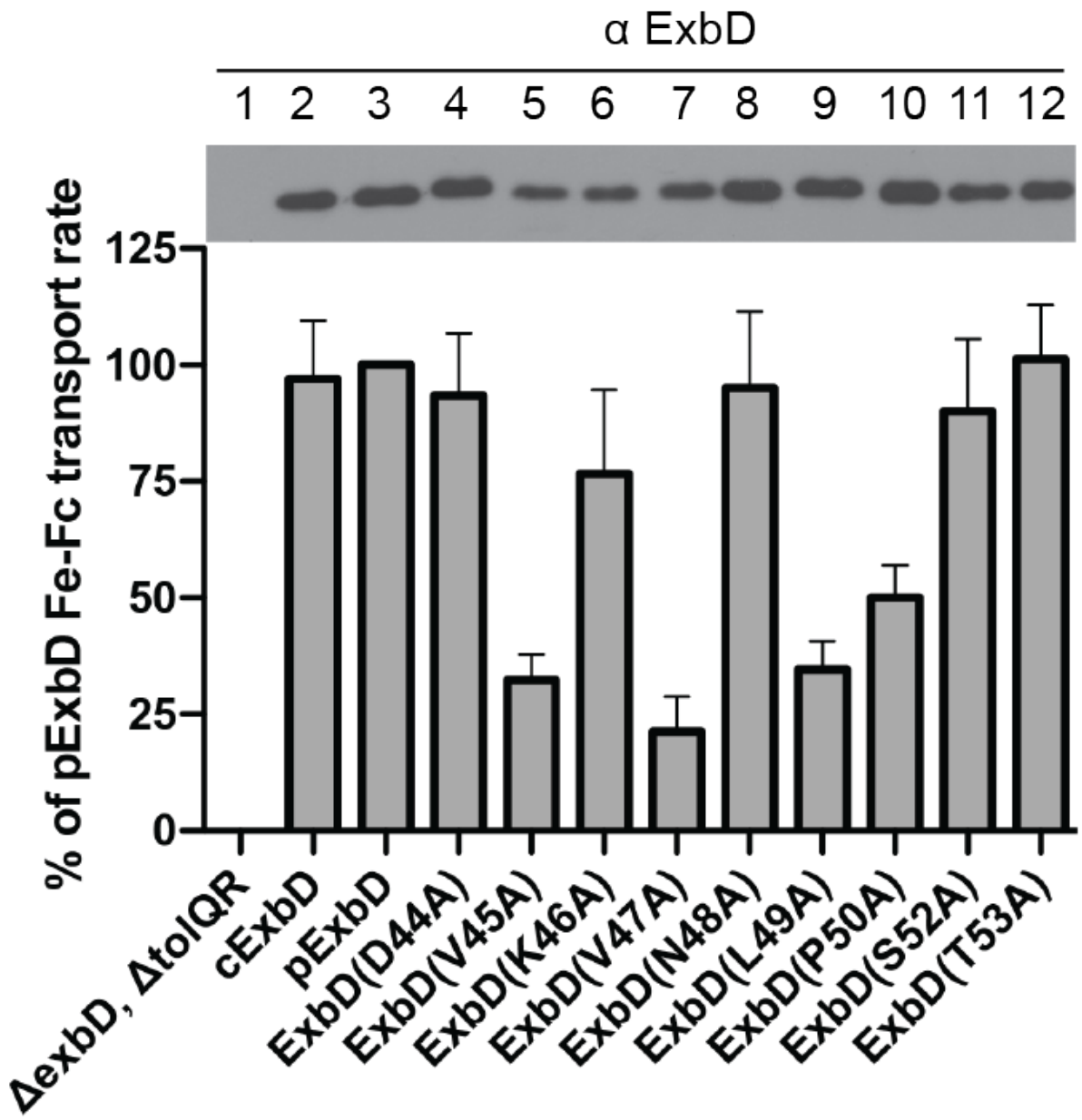

Figure S3: ExbD residues V45, V47, L49 and P50 are important for TonB System activity. Initial rate of ^{55}Fe-ferrichrome transport for ExbD single alanine substitutions in residues 44-53 and corresponding steady-state expression levels of the ExbD proteins**.** Strains were grown to mid-exponential phase and assayed as described in Methods and Materials. The percentages of activity were calculated relative to the initial rate of plasmid-encoded ExbD, pExbD (pKP999), expressed at chromosomal levels in RA1045 (Δ*exbD*, Δ*tolQR*). Assays were

1411 performed in triplicate and carried out at least twice for each strain. The slopes were
1412 determined by a linear regression fit of scintillation counts per minute. The error bars indicate
1413 mean ± SEM for a representative triplicate set. (above) Steady-state levels of ExbD-specific
1414 expression from the transport experiments are indicated above the corresponding bars of the
1415 graph below them. cExbD designates chromosomally expressed ExbD from the wild-type
1416 strain, W3110. All ExbD alanine substitution mutants are expressed from plasmids in RA1045
1417 (Δ*exbD*, Δ*tolQR*). The plasmid identities and concentrations of propionate for chromosomal
1418 expression are listed in Table S1. The mean percent of the pExbD ^{55}Fe-ferrichrome transport
1419 rates for ExbD (V45A), ExbD (V47A), ExbD (L49A), and ExbD (P50A) were 32%, 21%, 34%,
1420 and 50% respectively. ExbD residue 51 is naturally an alanine in *Escherichia coli* W3110 and
1421 is reflected in the pExbD initial rate.

1422
1423
1424
1425
1426
1427
1428
1429
1430
1431
1432
1433
1434
1435
1436
1437
1438

1439 **A.** **B.**

E. coli TolR(36–142)

	Chain 1	Chain 2
1	Gln-41(N)	Thr-139(OG1)
2	Val-43(N)	Leu-137(O)
3	Val-45(N)	Val-135(O)
4	Asp-46(N)	Asp-46(O)
5	Leu-47(N)	Lys-133(O)
6	Tyr-117(N)	Lys-133(O)
7	Tyr-117(N)	Val-115(O)
8	Tyr-117(OH)	Ile-109(O)
9	Asp-118(N)	Lys-113(O)
10	His-128(NE2)	Leu-47(O)
11	Ser-134(OG)	Asp-46(OD1)
12	Val-135(N)	Glu-44(OE2)
13	Val-135(N)	Val-45(O)
14	Leu-137(N)	Val-43(O)
15	Met-138(N)	Tyr-117(OH)
16	Thr-139(N)	Gln-41(O)
17	Thr-139(OG1)	Gln-41(O)
18	Thr-139(OG1)	Gln-41(N)
19	Leu-137(O)	Val-43(N)
20	Val-135(O)	Val-45(N)
21	Asp-46(O)	Asp-46(N)
22	Lys-133(O)	Leu-47(N)
23	Val-115(O)	Tyr-117(N)
24	Lys-113(O)	Tyr-117(N)
25	Ile-109(O)	Tyr-117(OH)
26	Lys-113(O)	Asp-118(N)
27	Leu-47(O)	His-128(NE2)
28	Asp-46(OD1)	Ser-134(OG)
29	Val-45(O)	Val-135(N)
30	Glu-44(OE2)	Val-135(N)
31	Val-43(O)	Leu-137(N)
32	Tyr-117(OH)	Met-138(N)
33	Gln-41(O)	Thr-139(N)
34	Gln-41(O)	Thr-139(OG1)
35a	His-128(NE2)	Asp-49(OD1)
36a	Asp-49(OD1)	His-128(NE2)

1440

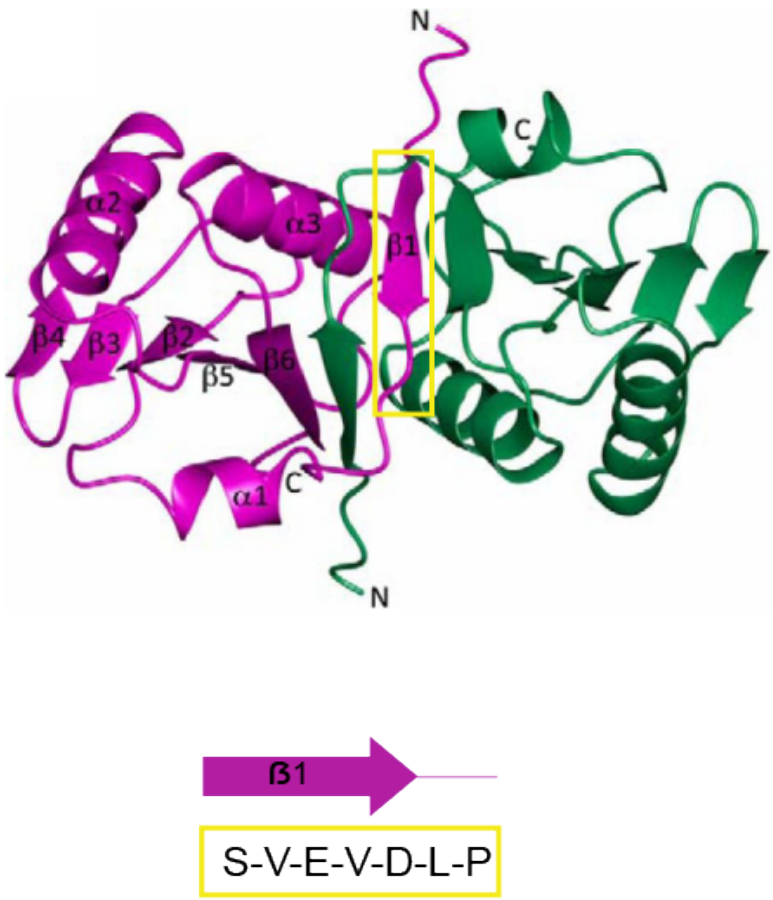

1441

1442 **Figure S4: The hydrophobic residues in ΨXΨXLP motif are located at dimeric interface**

1443 **of a TolR (36-142) dimeric crystal structure.** (A) The table of the TolR residues at the

1444 homodimeric interface. Chain 1 is one TolR and chain 2 is a second TolR. The red text

1445 identifies the conserved hydrophobic residues in the ΨXΨXLP motif from chain 1 and the blue

1446 text identifies the conserved hydrophobic residues in the ΨXΨXLP motif from chain 2. This

1447 table was adapted from Wojdyla et. al, 2015 [(7), B, top image] The dimeric crystal structure of

1448 TolR (36-142). The yellow rectangle identifies approximately where the motif lies from one

1449 TolR of the homodimeric structure. This structure was adapted from Wojdyla et. al, 2015 [(7),

1450 B, bottom image] The portion of one TolR where the motif residues lie. The conserved

1451 hydrophobic valines are in a beta strand and the conserved leucine and proline lie in a turn
1452 immediately distal to that beta-strand.

1453

1454 **Supplemental references:**

1455 1. Hill CW, Harnish BW. 1981. Inversions between ribosomal RNA genes of Escherichia coli.
1456 Proc Natl Acad Sci U S A 78:7069–7072.

1457 2. Larsen RA, Thomas MG, Postle K. 1999. Protonmotive force, ExbB and ligand-bound
1458 FepA drive conformational changes in TonB. Molecular Microbiology 31:1809–1824.

1459 3. Brinkman KK, Larsen RA. 2008. Interactions of the Energy Transducer TonB with
1460 Noncognate Energy-Harvesting Complexes. J Bacteriol 190:421–427.

1461 4. Larsen RA, Deckert GE, Kastead KA, Devanathan S, Keller KL, Postle K. 2007. His20
1462 Provides the Sole Functionally Significant Side Chain in the Essential TonB
1463 Transmembrane Domain. J Bacteriol 189:2825–2833.

1464 5. Ollis AA, Manning M, Held KG, Postle K. 2009. Cytoplasmic Membrane Protonmotive
1465 Force Energizes Periplasmic Interactions between ExbD and TonB. Mol Microbiol
1466 73:466–481.

1467 6. Young TS, Ahmad I, Yin JA, Schultz PG. 2010. An Enhanced System for Unnatural Amino
1468 Acid Mutagenesis in E. coli. Journal of Molecular Biology 395:361–374.

1469 7. Wojdyla JA, Cutts E, Kaminska R, Papadakos G, Hopper JTS, Stansfeld PJ, Staunton D,
1470 Robinson CV, Kleanthous C. 2015. Structure and Function of the Escherichia coli Tol-Pal
1471 Stator Protein TolR. J Biol Chem 290:26675–26687.